BACHELOR'S THESIS

The Anomalous Magnetic Moment of the Muon in the Two-Higgs-Doublet Model

Submitted by
Jannis Brirup

September 16, 2024

First examiner
Prof. Dr. Michael Klasen

Second examiner
PD Dr. Karol Kovařík

University of Münster
Institute for Theoretical Physics

Contents

1 Introduction

The Standard Model (SM), introduced in the late 20th century, effectively explains particle interactions, supported by experimental evidence. It provides a unified framework for electromagnetic, weak, and strong interactions. The SM comprises three generations of quarks and leptons, vector gauge bosons for each interaction, and a scalar Higgs particle. It has accurately predicted various experimental findings, including the theoretical prediction of the W, Z, and Higgs bosons.

Despite its significant achievements, the current SM fails to explain certain phenomena. For instance, dark matter, hypothesized in cosmology and observed, among other methods, through the rotation curves of nearby galaxies, remains unexplained. Additional unresolved phenomena include dark energy, gravity, and the masses of neutrinos. A challenge to the SM is the phenomenon of baryon asymmetry. In particular, according to the SM, matter and antimatter should be symmetric, except for a minor violation in weak interactions that is not enough to account for this asymmetry [1].
Another possible sign of new physics beyond the Standard Model (BSM) is indicated by the muon's anomalous magnetic moment (AMM), $a_\mu \equiv (g_\mu - 2)/2$, where g_μ is the gyromagnetic factor (g-factor), also known as the Landé factor. It expresses the ratio between the muon's magnetic moment and the magnetic moment anticipated by classical physics, considering the associated angular momentum. Consequently, the muon's spin results in the magnetic moment

$$\vec{\mu}_\mu = -g_\mu \frac{e}{2m_\mu}\vec{S}.$$

Exploring relativistic quantum mechanics using the Dirac equation yields the result $g = 2$. In the SM, the anomaly is calculable through corrections from quantum electrodynamics (QED), quantum chromodynamics (QCD), and electroweak interactions, leading to $a_\mu^{\mathrm{SM}} = 116\,591\,810(43) \times 10^{-11}$ [2]. In August 2023, the muon $(g-2)$ collaboration at Fermi National Accelerator Laboratory announced an experimental value even more precise than their previous measurement [3, 4]. Combined with the measurement from the Brookhaven $(g-2)$ collaboration [5] this gives a world average for the experimental value $a_\mu^{\mathrm{exp}} = 116\,592\,059(22) \times 10^{-11}$. The discrepancy between the theoretical and experimental value is given by

$$\Delta a_\mu = a_\mu^{\mathrm{exp}} - a_\mu^{\mathrm{SM}} = (249 \pm 48) \times 10^{-11}.$$

This 5.1σ deviation underscores the importance of studying the muon's AMM to potentially uncover new physics, the focus of this thesis.

Therefore, $g = 2$ is derived both by transforming the Dirac equation into the Pauli equation and by calculating the invariant amplitude $\mathcal{M}$ at tree level. The invariant amplitude can be represented by different form factors that are used to determine the AMM. Then, the dominant one-loop QED correction to the AMM is calculated. In addition, general electroweak one-loop contributions are considered, which include both fermions and scalars and are applicable to arbitrary models. A distinction is made between the topology in which the photoemission comes from an internal charged fermion line and that in which the photoemission takes place at an internal charged scalar line. The former is calculated analytically in this thesis; both cases are derived in *Mathematica* using the open source *Package*-`X` [6]. The resulting integral equation depends on general parameters, applicable

for arbitrary models.
This thesis considers the extension of the SM with the two-Higgs-doublet model (2HDM), which leads to the existence of four scalar Higgs particles instead of one. The 2HDM is used in supersymmetric frameworks, such as the Minimal Supersymmetric Standard Model (MSSM) [7]. Additionally, by selecting complex parameters, a source for the CP-violation can be identified, potentially elucidating the previously mentioned baryon asymmetry in the universe [8]. The aim of this thesis is to investigate the contribution of the new particles to the AMM. By adjusting various parameters, such as the masses of the new scalars or coupling constants, the theoretical AMM value can be aligned with the experimental results. Specifically, different structures of the Yukawa coupling matrices are considered and analyzed.

2 The Magnetic Moment of the Muon in the Standard Model

Non-relativistic we can derive the magnetic moment of a circular current I by

$$\vec{\mu} = IA\ \vec{n}_A, \tag{2.0.1}$$

where $\vec{n}_A$ is the normal vector of the area A enclosed by the current. As an illustration, consider a single particle that has charge q, mass m and velocity v on a circular path with radius r. With orbital angular momentum $\vec{L}$ and period duration T, the magnetic moment can be defined using $I = q/T$ and $T = 2\pi r/v$ as follows:

$$\vec{\mu} = \frac{q}{2m}\vec{L}. \tag{2.0.2}$$

In addition to the orbital angular momentum, particles have an intrinsic angular momentum, called spin. This has no classical analogue. A relativistic consideration using Dirac's equation shows that the spin contributes twice as much to the magnetic moment as the orbital angular momentum discussed earlier. This relative factor ($g = 2$) will be derived in the following.

2.1 From the Dirac Equation to the Pauli Equation

In non-relativistic quantum mechanics, the dynamics of a state Ψ is described by the Schrödinger equation with the non-relativistic Hamilton Operator:

$$i\hbar\frac{\partial}{\partial t}\Psi = H\Psi = \Big(\frac{\vec{p}^2}{2m} + V(\vec{x}, t)\Big)\Psi. \tag{2.1.1}$$

However, this is not Lorentz covariant (recognizable by different orders of time and space derivatives in spatial representation) and loses its validity at velocities close to the speed of light c. This section is based on [9, 10]. From this point forward, natural units are adopted, which implies $\hbar = c = 1$.

The transition to relativistic quantum mechanics was achieved in 1926 via the Klein-Gordon equation, named after the physicists Oskar Klein and Walter Gordon, which is based on the relativistic energy-momentum relationship:

$$p^\mu p_\mu = m^2. \tag{2.1.2}$$

According to the correspondence principle, the contravariant four-gradient can represent the four-momentum as follows:

$$p^\mu \to i\partial^\mu, \qquad \text{with} \qquad \partial^\mu = \left(\frac{\partial}{\partial t}, -\vec{\nabla}\right).$$

From Eq. (2.1.2), the Klein-Gordon equation is derived:

$$\left(\Delta - \frac{\partial^2}{\partial t^2} - m^2\right)\Psi = 0. \tag{2.1.3}$$

Because the wave function is a scalar quantity, it is only applicable to describe spinless particles. On the other hand, particles possessing an intrinsic angular momentum necessitate a representation through spinors. In 1927, Dirac formulated an equation that is linear in its derivatives with respect to both time and space. The shift from the Klein-Gordon

equation to the Dirac equation is achieved via linearization. Consequently, the ansatz for the Dirac Hamilton operator H_D is given by

$$H_D^2\psi = (\alpha_i p_i + \beta m)(\alpha_j p_j + \beta m)\psi, \tag{2.1.4}$$

where the indices can take on the values $i, j = 1, 2, 3$. Compared with the Klein-Gordon equation, the ensuing conditions for the newly introduced coefficients α_i and β are obtained:

$$\{\alpha_i, \alpha_j\} = 2\delta_{ij}, \qquad \{\alpha_i, \beta\} = 0, \qquad \beta^2 = 1, \tag{2.1.5}$$

where $\{,\}$ denotes the anticommutator. The Dirac Hamiltonian can be expressed as

$$H_D = -i\vec{\alpha} \cdot \vec{\nabla} + \beta m, \tag{2.1.6}$$

which results in the Dirac equation:

$$\left(i\frac{\partial}{\partial t} + i\vec{\alpha} \cdot \vec{\nabla} - \beta m\right)\psi = 0. \tag{2.1.7}$$

For a particle with charge $q = -e$ in an electromagnetic potential we employ the substitution $p^\mu \to p^\mu + eA^\mu$. Here, $A^\mu = (\Phi, \vec{A})$ is the contravariant four-potential with the scalar potential Φ and the vector potential $\vec{A}$. The Dirac equation in an electromagnetic field is then given by

$$\left(i\frac{\partial}{\partial t} + \vec{\alpha} \cdot (i\vec{\nabla} - e\vec{A}) - \beta m + e\Phi\right)\psi = 0. \tag{2.1.8}$$

The Dirac operator in an electromagnetic field can be identified as

$$H_D^{\mathrm{EM}} = \vec{\alpha} \cdot (\vec{p} + e\vec{A}) + \beta m - e\Phi. \tag{2.1.9}$$

Different sets of $\vec{\alpha}$ and β can satisfy the conditions mentioned in Eq. (2.1.5). A possible choice is given by the Dirac representation:

$$\vec{\alpha} = \begin{pmatrix} 0 & \vec{\sigma} \\ \vec{\sigma} & 0 \end{pmatrix}, \quad \beta = \begin{pmatrix} \mathbb{I}_2 & 0 \\ 0 & -\mathbb{I}_2 \end{pmatrix}. \tag{2.1.10}$$

Another option is the Weyl representation:

$$\vec{\alpha} = \begin{pmatrix} -\vec{\sigma} & 0 \\ 0 & \vec{\sigma} \end{pmatrix}, \quad \beta = \begin{pmatrix} 0 & \mathbb{I}_2 \\ \mathbb{I}_2 & 0 \end{pmatrix}. \tag{2.1.11}$$

The vector $\vec{\sigma}$ with three components is constructed using the 2×2 Pauli matrices as its elements:

$$\sigma_1 = \begin{pmatrix} 0 & 1 \\ 1 & 0 \end{pmatrix}, \qquad \sigma_2 = \begin{pmatrix} 0 & -i \\ i & 0 \end{pmatrix}, \qquad \sigma_3 = \begin{pmatrix} 1 & 0 \\ 0 & -1 \end{pmatrix}. \tag{2.1.12}$$

Since $\vec{\alpha}$ and β are 4×4 matrices, ψ is a four-component spinor, called Dirac spinor. In the following, this will be expressed by two two-component spinors. These contain the upper two and the lower two components, respectively:

$$\psi = \begin{pmatrix} \varphi \\ 0 \end{pmatrix} + \begin{pmatrix} 0 \\ \chi \end{pmatrix}. \tag{2.1.13}$$

Using the Dirac operator for a massive particle with negative charge in an electromagnetic field, as referred to in Eq. (2.1.9), and employing the Dirac representation, we derive

$$\begin{aligned} H_D^{\mathrm{EM}} \begin{pmatrix} \varphi \\ \chi \end{pmatrix} =& \begin{pmatrix} 0 & \vec{\sigma} \cdot (\vec{p} + e\vec{A}) \\ \vec{\sigma} \cdot (\vec{p} + e\vec{A}) & 0 \end{pmatrix} \begin{pmatrix} \varphi \\ \chi \end{pmatrix} \\ &+ m \begin{pmatrix} \mathbb{I}_2 & 0 \\ 0 & -\mathbb{I}_2 \end{pmatrix} \begin{pmatrix} \varphi \\ \chi \end{pmatrix} - e\Phi \begin{pmatrix} \varphi \\ \chi \end{pmatrix} \\ =& (\vec{p} + e\vec{A}) \cdot \begin{pmatrix} \vec{\sigma}\chi \\ \vec{\sigma}\varphi \end{pmatrix} + m \begin{pmatrix} \varphi \\ -\chi \end{pmatrix} - e\Phi \begin{pmatrix} \varphi \\ \chi \end{pmatrix} = E \begin{pmatrix} \varphi \\ \chi \end{pmatrix}. \end{aligned} \tag{2.1.14}$$

This leads to a system of two coupled two-component equations:

$$(E - m + e\Phi)\varphi = (\vec{p} + e\vec{A}) \cdot \vec{\sigma}\chi, \tag{2.1.15}$$

$$(E + m + e\Phi)\chi = (\vec{p} + e\vec{A}) \cdot \vec{\sigma}\varphi. \tag{2.1.16}$$

Within the Weyl representation, it becomes evident that the mass determines the coupling between the left-handed (upper two components of the spinor) and right-handed (lower two components of the spinor) Weyl spinors. However, the choice of the Dirac representation is advantageous here because it diagonalizes the energy in the non-relativistic limit. If we consider this limit, we can approach the Pauli theory, in which the total energy E is approximately equal to the rest energy m and the scalar potential Φ becomes negligible:

$$E \approx m, \qquad\qquad m \gg e\Phi.$$

Under these approximations, Equation (2.1.16) can be written as:

$$\chi \approx \frac{1}{2m}(\vec{p} + e\vec{A}) \cdot \vec{\sigma}\varphi. \tag{2.1.17}$$

In the non-relativistic limit, it is evident that χ is significantly smaller than φ. By substituting the expression for χ into Eq. (2.1.15), we derive

$$H_P\varphi = (E - m)\varphi, \tag{2.1.18}$$

with

$$H_P = \frac{1}{2m}[(\vec{p} + e\vec{A}) \cdot \vec{\sigma}][(\vec{p} + e\vec{A}) \cdot \vec{\sigma}] - e\Phi\mathbb{I}_2. \tag{2.1.19}$$

The expression can be further evaluated as

$$\begin{aligned} [(\vec{p} + e\vec{A}) \cdot \vec{\sigma}][(\vec{p} + e\vec{A}) \cdot \vec{\sigma}] =& (p + eA)_i(p + eA)_j\sigma_i\sigma_j \\ =& (p + eA)_i(p + eA)_j(\delta_{ij}\mathbb{I}_2 + i\epsilon_{ijk}\sigma_k) \\ =& (p + eA)_i(p + eA)_i + i\epsilon_{ijk}(p + eA)_i(p + eA)_j\sigma_k \\ =& (\vec{p} + e\vec{A})^2\mathbb{I}_2 + i\vec{\sigma} \cdot [(\vec{p} + e\vec{A}) \times (\vec{p} + e\vec{A})], \end{aligned} \tag{2.1.20}$$

where in the final step, the fact that the Pauli matrices commute with momentum and the vector potential is used.
The second term yields the magnetic field that can be identified with the correspondence $\vec{p} \to -i\vec{\nabla}$. We apply this to φ and obtain

$$[(\vec{p} + e\vec{A}) \times (\vec{p} + e\vec{A})]\varphi = [e(\vec{p} \times \vec{A} + \vec{A} \times \vec{p})]\varphi$$

$$
\begin{aligned}
&= -ie[\vec{\nabla} \times (\vec{A}\phi) + \vec{A} \times (\vec{\nabla}\varphi)] \\
&= -ie[(\vec{\nabla} \times \vec{A})\phi - \vec{A} \times (\vec{\nabla}\varphi) + \vec{A} \times (\vec{\nabla}\varphi)] \\
&= -ie\vec{B}\varphi, \qquad (2.1.21)
\end{aligned}
$$

where the identity $\vec{\nabla} \times (\vec{A}\phi) = (\vec{\nabla} \times \vec{A})\phi - \vec{A} \times (\vec{\nabla}\phi)$ is used. The magnetic field is given by $\vec{B} = \mathrm{rot}\vec{A}$. Inserting Eq. (2.1.20) and Eq. (2.1.21) in Eq. (2.1.19), the Pauli Hamilton Operator takes the form

$$H_P = \left[\frac{1}{2m}(\vec{p} + e\vec{A})^2 - e\Phi\right] \mathbb{I}_2 + \frac{e}{2m}\vec{\sigma} \cdot \vec{B}.$$

In the Dirac formalism, a 4-component theory is considered, whereas the Pauli formalism involves 2-component spinors, each representing the particle's spin. Using the definition of the magnetic moment, we deduce $g = 2$ with $\vec{\mu} = -\frac{g}{2}\frac{e}{2m}\vec{\sigma}$. The following steps demonstrate that the g-factor represents the relative strength of its intrinsic magnetic dipole moment to the spin-orbital coupling strength. The Pauli Hamiltonian can be expressed as

$$H_P = \left(\frac{\vec{p}^2}{2m} + \frac{e^2\vec{A}^2}{2m} + \frac{e}{2m}(\vec{p} \cdot \vec{A} + \vec{A} \cdot \vec{p}) - e\Phi\right) \mathbb{I}_2 + \frac{e}{2m}\vec{\sigma} \cdot \vec{B}. \qquad (2.1.22)$$

Using Appendix A.1, it follows that:

$$\vec{p} \cdot \vec{A} = [\vec{p}, \vec{A}] + \vec{A} \cdot \vec{p} = -i\vec{\nabla} \cdot \vec{A} + \vec{A} \cdot \vec{p}.$$

By selecting the Coulomb gauge, characterized by the condition $\vec{\nabla} \cdot \vec{A} = 0$, one derives

$$H_P = \left(\frac{\vec{p}^2}{2m} + \frac{e^2\vec{A}^2}{2m} + \frac{e}{m}\vec{A} \cdot \vec{p} - e\Phi\right) \mathbb{I}_2 + \frac{e}{2m}\vec{\sigma} \cdot \vec{B}.$$

The vector potential can be chosen as $\vec{A} = \frac{1}{2}\vec{B} \times \vec{r}$. This selection satisfies the Coulomb gauge condition and generates a homogeneous magnetic field $\vec{B}$:

$$\vec{\nabla} \cdot \vec{A} = \partial_i A_i = \frac{1}{2}\partial_i \epsilon_{ijk} B_j x_k = \frac{1}{2}\epsilon_{ijk}\delta_{ik}B_j = 0, \qquad (2.1.23)$$

$$
\begin{aligned}
[\mathrm{rot}\vec{A}]_i = \epsilon_{ijk}\partial_j A_k &= \epsilon_{ijk}\partial_j \frac{1}{2}\epsilon_{klm}B_l x_m \\
&= \frac{1}{2}\epsilon_{ijk}\delta_{jm}\epsilon_{klm}B_l \\
&= \frac{1}{2}\underbrace{\epsilon_{ijk}\epsilon_{ljk}}_{=2\delta_{il}} B_l = B_i. \qquad (2.1.24)
\end{aligned}
$$

Substituting the form of the vector potential in the Pauli Hamiltonian yields

$$H_P = \left(\frac{\vec{p}^2}{2m} + \frac{e^2\vec{A}^2}{2m} + \frac{e}{2m}(\vec{B} \times \vec{r}) \cdot \vec{p} - e\Phi\right) \mathbb{I}_2 + \frac{e}{2m}\vec{\sigma} \cdot \vec{B}.$$

Given that $(\vec{B} \times \vec{r}) \cdot \vec{p} = (\vec{r} \times \vec{p}) \cdot \vec{B} = \vec{L} \cdot \vec{B}$, the orbital angular momentum $\vec{L}$ can be identified, leading to the Pauli Hamiltonian in its final form:

$$H_P = \left[\frac{\vec{p}^2}{2m} + \frac{e^2\vec{A}^2}{2m} - e\Phi\right] \mathbb{I} + \underbrace{\frac{e}{2m}(\vec{L} + 2\vec{S})}_{=-\vec{\mu}} \cdot \vec{B}. \qquad (2.1.25)$$

The spin operator is given by $\vec{S} = \vec{\sigma}/2$, which consequently results in the spin coupling being precisely twice that of the orbital coupling, characterized by the gyromagnetic factor $g = 2$. This prediction was a significant triumph of the Dirac equation.

2.2 Tree-level Contribution

The following section will analyze the interaction of a muon with the electromagnetic field A^μ using first-order perturbation theory. Consequently, this results in $g = 2$ in leading order and gives insight into the origin of the magnetic moment. Since only the muon mass m_μ is involved in the next sections, we omit the index for simplicity ($m \equiv m_\mu$). This section is based on [9, pp. 117–119].

The starting point is the covariant form of the Dirac equation (see Appendix A.2):

$$(\not{p} - m)\psi = 0, \tag{2.2.1}$$

where the Dirac slash notation was introduced with $\not{p} = \gamma_\mu p^\mu$. For the muon in an electromagnetic field A^μ, the substitution $p^\mu \to p^\mu + eA^\mu$ is performed. This leads to

$$(\gamma^\mu p_\mu - m)\psi = -e\gamma^\mu A_\mu \psi \equiv \gamma^0 V \psi. \tag{2.2.2}$$

It becomes evident that incorporating γ^0 results in the inclusion of the perturbation potential V (e.g., $-e\Phi$ for the timelike component) in the same way as in the Schrödinger equation. The transition amplitude between the final state ψ_2 and the initial state ψ_1 can be determined using time-dependent perturbation theory. The first order transition amplitude is given by

$$\begin{aligned}\mathcal{T}_{21} &= -i \int \psi_2^\dagger V \psi_1 \, d^4x \\ &= ie \int \bar{\psi}_2 \gamma^\mu A_\mu \psi_1 \, d^4x \\ &= -i \int j_{21}^\mu A_\mu \, d^4x,\end{aligned} \tag{2.2.3}$$

where $\bar{\psi} = \psi^\dagger \gamma^0$ and $(\gamma^0)^2 = \mathbb{I}_4$ was used. Additionally, the transition current between the initial and final state is defined as

$$j_{21}^\mu \equiv -e\bar{\psi}_2 \gamma^\mu \psi_1 = -e\bar{u}(q_2)\gamma^\mu u(q_1) e^{i(q_2 - q_1)\cdot x}. \tag{2.2.4}$$

The undisturbed states (free particles with momentum q) were written as plane wave solutions with a four-component spatially independent spinor $u(q)$:

$$\psi(x) = u(q) e^{-iq\cdot x}. \tag{2.2.5}$$

It should be noted that a transition current of $j_{21}^\mu = -e(q_1 + q_1)^\mu e^{i(q_2 - q_1)\cdot x}$ follows from the Klein-Gordon equation, which describes spinless particles. It turns out that this difference implies that charged spin-1/2 particles, in contrast to charged spinless particles, interact with the electromagnetic field A^μ via both their charge and their magnetic moment. This will be investigated in the following. Using the Gordon identity (proven in Appendix A.3)

$$\bar{u}(q_2)\gamma^\mu u(q_1) = \frac{1}{2m}\bar{u}(q_2)\Big[(q_1 + q_2)^\mu + i\sigma^{\mu\nu}(q_2 - q_1)_\nu\Big]u(q_1), \tag{2.2.6}$$

the transmission amplitude with $p^\mu = q_2^\mu - q_1^\mu$ results in:

$$\begin{aligned}\mathcal{T}_{21} =& -i \int j^\mu A_\mu \, d^4x \\ =& ie \int \bar{u}(q_2)\gamma^\mu A_\mu e^{ip\cdot x} u(q_1) \, d^4x\end{aligned}$$

$$
\begin{aligned}
=&\frac{ie}{2m}\int e^{ip_0 t}\,dt\int \bar{u}(q_2)\Big[(q_1+q_2)^\mu + i\sigma^{\mu\nu}(q_2-q_1)_\nu\Big]u(q_1)e^{-i\vec{p}\cdot\vec{x}}A_\mu\,d^3x\\
=&-2\pi i\delta(p_0)\Big[\underbrace{\int -\frac{e}{2m}\bar{u}(q_2)(q_1+q_2)^\mu u(q_1)e^{-i\vec{p}\cdot\vec{x}}A_\mu\,d^3x}_{\text{(I)}}\\
&\qquad\qquad+\underbrace{\int -\frac{e}{2m}\bar{u}(q_2)i\sigma^{\mu\nu}(q_2-q_1)_\nu u(q_1)e^{-i\vec{q}\cdot\vec{x}}A_\mu\,d^3x}_{\text{(II)}}\Big]. \qquad (2.2.7)
\end{aligned}
$$

The δ-function thus indicates conservation of energy between final and initial state. Both marked terms are discussed in the following.
In integral (I) the spacial components vanish. To show this, we change the indices to $i,j=1,2,3$ and only use lower indices. The spatial components of the metric tensor (in Minkowski space) form a negative identity matrix $-\mathbb{I}_3$, resulting in:

$$
\begin{aligned}
(\mathrm{I})_{\text{spacial}} &= \int -\frac{e}{2m}\bar{u}(q_2)e^{-i\vec{q}_2\cdot\vec{x}}(q_1+q_2)_i u(q_1)e^{i\vec{q}_1\cdot\vec{x}}(-\delta_{ij}A_j)\,d^3x\\
&= \int \frac{e}{2m}\bar{u}(q_2)i\partial_i(e^{-i\vec{q}_2\cdot\vec{x}}-e^{i\vec{q}_1\cdot\vec{x}})u(q_1)A_i\,d^3x\\
&= \int i\frac{e}{2m}\bar{u}(q_2)u(q_1)\partial_i\Big[(e^{-i\vec{q}_2\cdot\vec{x}}-e^{i\vec{q}_1\cdot\vec{x}})A_i\Big]\,d^3x\\
&\qquad\qquad -\int i\frac{e}{2m}\bar{u}(q_2)u(q_1)(e^{-i\vec{q}_2\cdot\vec{x}}-e^{i\vec{q}_1\cdot\vec{x}})\partial_i A_i\,d^3x\\
&= \int i\frac{e}{2m}\bar{u}(q_2)u(q_1)\Big[(e^{-i\vec{q}_2\cdot\vec{x}}-e^{i\vec{q}_1\cdot\vec{x}})\vec{A}\Big]\cdot d\vec{S}\\
&\qquad\qquad -\int i\frac{e}{2m}\bar{u}(q_2)u(q_1)(e^{-i\vec{q}_2\cdot\vec{x}}-e^{i\vec{q}_1\cdot\vec{x}})\vec{\nabla}\cdot\vec{A}\,d^3x=0
\end{aligned}
$$

Since the complex exponential functions are bounded, and under the assumption $\vec{A}$ vanishes as $x\to\infty$, the first term becomes zero. With the choice of the Coulomb Gauge ($\vec{\nabla}\cdot\vec{A}=0$) the second term also vanishes.

Thus, we only need to consider the timelike component. Employing the δ-function in the non-relativistic regime, where the total energy E is nearly equal to the rest energy m, we obtain:

$$
\begin{aligned}
(\mathrm{I})_{\text{time}} &= \int -\frac{e}{2m}\bar{u}(q_2)(q_1+q_2)^0\mathbb{I}_4 u(q_1)e^{-i\vec{p}\cdot\vec{x}}\Phi\,d^3x\\
&= \int -\frac{e}{2m}\bar{u}(q_2)(2q_1^0)\mathbb{I}_4 u(q_1)e^{-i\vec{p}\cdot\vec{x}}\Phi\,d^3x\\
&\approx \int -e\bar{u}_A(q_2)e^{-i\vec{q}_2\cdot\vec{x}}\mathbb{I}_2 e^{i\vec{q}_1\cdot\vec{x}}u_A(q_1)\Phi\,d^3x\\
&= \int \bar{\psi}_2^A(\vec{x})(-e\Phi\mathbb{I}_2)\psi_1^A(\vec{x})\,d^3x.
\end{aligned}
$$

Here, $\psi_i^A(\vec{x})=u_A(q_i)e^{i\vec{q}_i\cdot\vec{x}}$ is introduced, where the index A describes the (in the non-relativistic limit) large 2-component spinor.
In the second term, denoted as (II), the timelike component vanishes due to the δ-function in Eq. (2.2.7). As a result, we modify the indices to $i,j=1,2,3$ and move on to the Euclidean metric. The remaining spatial components are given by:

$$
(\mathrm{II}) = \int -\frac{e}{2m}\bar{u}(q_2)i\sigma_{ij}\Big[-\delta_{jk}(q_2-q_1)_k\Big]e^{-i\vec{p}\cdot\vec{x}}(-\delta_{il}A_l)u(q_1)\,d^3x
$$

$$
\begin{aligned}
&= \int \frac{e}{2m}\bar{u}(q_2) i\sigma_{ij}\left(\frac{\partial_j}{i}e^{-i\vec{p}\cdot\vec{x}}\right) A_i u(q_1)\, d^3x \\
&= \int \frac{e}{2m}\bar{u}(q_2)\sigma_{ij}\partial_j\left(e^{-i\vec{p}\cdot\vec{x}}A_i\right)u(q_1)\, d^3x - \int \frac{e}{2m}\bar{u}(q_2)\sigma_{ij}e^{-i\vec{p}\cdot\vec{x}}(\partial_j A_i)u(q_1)\, d^3x \\
&\overset{(A.4)}{\approx} \int \frac{e}{2m}\bar{u}_A(q_2)\epsilon_{ijk}\sigma_k\partial_j\left(e^{-i\vec{p}\cdot\vec{x}}A_i\right)u_A(q_1)\, d^3x - \int \frac{e}{2m}\bar{u}_A(q_2)\epsilon_{ijk}\sigma_k e^{-i\vec{p}\cdot\vec{x}}(\partial_j A_i)u_A(q_1)\, d^3x \\
&= \int -\frac{e}{2m}\bar{u}_A(q_2)\vec{\sigma}\cdot\left[\vec{\nabla}\times\left(e^{-i\vec{p}\cdot\vec{x}}\vec{A}\right)\right]u_A(q_1) + \int \frac{e}{2m}\bar{u}_A(q_2)\vec{\sigma}\cdot\left[\vec{\nabla}\times\vec{A}\right]e^{-i\vec{p}\cdot\vec{x}}u_A(q_1)\, d^3x \\
&= \int -\frac{e}{2m}\bar{u}_A(q_2)\mathrm{div}\left[\left(e^{-i\vec{p}\cdot\vec{x}}\vec{A}\right)\times\vec{\sigma}\right]u_A(q_1)\, d^3x + \int \frac{e}{2m}\bar{u}_A(q_2)\vec{\sigma}\cdot\vec{B}u_A(q_1)e^{-i\vec{p}\cdot\vec{x}}\, d^3x.
\end{aligned}
$$

Here, the relation shown in Appendix A.4 was used for the commutator of the gamma matrices. In the final step, we applied

$$
\vec{\sigma}\cdot\mathrm{rot}\left[e^{-i\vec{p}\cdot\vec{x}}\vec{A}\right] = \mathrm{div}\left[\left(e^{-i\vec{p}\cdot\vec{x}}\vec{A}\right)\times\vec{\sigma}\right] + e^{-i\vec{p}\cdot\vec{x}}\vec{A}\cdot\mathrm{rot}\left[\vec{\sigma}\right] = \mathrm{div}\left[\left(e^{-i\vec{p}\cdot\vec{x}}\vec{A}\right)\times\vec{\sigma}\right].
$$

Considering that the vector potential $\vec{A}(\vec{x})$ vanishes as $\vec{x}\to\infty$, the application of Gauss's theorem allows us to nullify the first term, resulting in

$$
\int\left[-\frac{e}{2m}\bar{\psi}_2(\vec{x})i\sigma^{\mu\nu}\left(q_2-q_1\right)_\nu\psi_1(\vec{x})\right]A_\mu\, d^3x = \int\frac{e}{2m}\bar{\psi}_2^A(\vec{x})\vec{\sigma}\cdot\vec{B}\psi_1^A(\vec{x})\, d^3x.
$$

The first-order perturbation amplitude in the non-relativistic limit is therefore given by

$$
\mathcal{T}_{21} = -2\pi i\delta(p_0)\left[\int\bar{\psi}_2^A(\vec{x})\left(-e\Phi\mathbb{I}_2+\frac{e}{2m}\vec{\sigma}\cdot\vec{B}\right)\psi_1^A(\vec{x})\, d^3x\right].
$$

The result is cross-checked with the amplitude in the literature [9, p. 135]. It is evident from the structure of the Pauli Hamiltonian in Eq. (2.1.25) that the relevant interaction terms arising from both the charge and the magnetic moment are included. Comparing the previously mentioned transition currents for a spinless (scalar) particle to those for a spin-$\frac{1}{2}$ fermion reveals that in the scalar particle scenario, only the term $-e\Phi$ is present, whereas, in the fermion scenario, there is an additional interaction with the magnetic field.

At the end of this section, the transition to the invariant amplitude $\mathcal{M}$ will be made. The calculation of the first-order perturbation theory considered above corresponds to the tree-level Feynman diagram:

$$
i\mathcal{M}^\mu =
$$

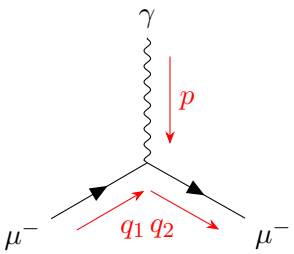

$$
= -ie\bar{u}(q_2)\gamma^\mu u(q_1), \tag{2.2.8}
$$

where, due to the incoming photon with polarization vector ϵ_μ, the invariant amplitude is given by $\mathcal{M} = \epsilon_\mu\mathcal{M}^\mu$. In the following, this will be briefly motivated by quantum field theory. This forms a more fundamental and uniform description between particles and fields. Instead of using the wave functions of the individual particles, quantum field theory is used to describe particles as an excitation of the corresponding quantum field. The initial state $|i\rangle$ and the final state $|f\rangle$ can be formulated using the second quantization:

$$
|i\rangle = |\mu^-_{s_1}(q_1),\gamma_\lambda(p)\rangle = \sqrt{2E_{q_1}}\sqrt{2E_p}\; a^{s_1\dagger}_{q_1}a^{\lambda\dagger}_p|0\rangle, \tag{2.2.9}
$$

$$|f\rangle = |\mu^-_{s_2}(q_2)\rangle = \sqrt{2E_{q_2}}\; a^{s_2\dagger}_{q_2}|0\rangle. \tag{2.2.10}$$

The operators $a_p^{s\dagger}$ ($a_p^{\lambda\dagger}$) generate a muon with spin s (photon with polarization λ) and momentum p. A possible convention and useful term in relation to Lorentz transformations is the factor $\sqrt{2E_p}$ with $E_p = \sqrt{\vec{p}^2 + m^2}$ [11]. In addition, $|0\rangle$ is the vacuum state, which is the lowest energy state. The first-order transition amplitude, motivated by Eq. (2.2.3) can thus be expressed using its quantum fields (see Appendix A.5):

$$\mathcal{T}_{if} = -iQ_F e \int d^4x\, \langle 0|a^{s_1}_{q_2}\bar{\psi}(x)\gamma^\mu\psi(x)A_\mu(x)a^{s_2\dagger}_{q_1}a^{\lambda\dagger}_p|0\rangle \prod_{i=q_1,q_2,p}\sqrt{2E_i}. \tag{2.2.11}$$

The annihilation operator $a^{s_1}_{q_2}$ occurs because it is the adjoint operator to the corresponding generating operator $a^{s_1\dagger}_{q_2}$. The commutation and anticommutation relations are crucial and are given in Appendix A.5. Note that an annihilation operator acting on a vacuum state leads to zero ($a|0\rangle = 0$). Writing out the fields and commute them with the creation and annihilation operators results in

$$\mathcal{T}_{if} = -iQ_F e \int d^4x\, \langle 0|e^{iq_2\cdot x}\bar{u}(q_2)\gamma^\mu e^{-ip\cdot x}\epsilon_\mu u(q_1)e^{-iq_1 x}|0\rangle, \tag{2.2.12}$$

whereby the spin and polarization indices have been omitted. Thus, the normalization $\langle 0|0\rangle = 1$ demonstrates that this description is equivalent to the one given in Eq. (2.2.3). After performing the integration, the invariant amplitude can be defined as follows:

$$\mathcal{T}_{if} = -i(2\pi)^4\delta^{(4)}(q_1 - q_2 + p)\underbrace{\epsilon_\mu(Q_F e\bar{u}(q_2)\gamma^\mu u(q_1))}_{\equiv\epsilon_\mu\mathcal{M}^\mu}. \tag{2.2.13}$$

The δ-function, which is extracted from the invariant amplitude, describes the conservation of momentum at the vertex. In Appendix A.6, the Feynman rules are outlined to derive the invariant amplitude from the respective Feynman diagram. The tree-level amplitude, as shown in Eq. (2.2.8), matches the invariant amplitude defined above.

With the help of Feynman diagrams and Feynman rules, the invariant amplitude can, in principle, be derived in any order of perturbation theory. Since the vertex correction, which leads to the anomalous magnetic moment, is included in this approach, Feynman amplitudes are considered in the following sections. It will turn out that each invariant amplitude is characterized by four different form factors, where one of those leads to the anomalous magnetic moment.
From this section, it is already understood that to determine the gyromagnetic factor, within the invariant amplitude $\mathcal{M}$, one needs to look for $-4m/e$ times the coefficient of $ip_\nu\bar{u}(q_2)\sigma^{\nu\mu}u(q_1)$. Thus, with the knowledge obtained from the Feynman diagram in Eq. (2.2.8) and the Gordon identity we can immediately derive $g = 2$ at tree level.

2.3 Form Factors

In the last section, it became clear that $g = 2$ follows from the tree-level Feynman diagram. The decisive aspect was the vertex factor with interaction with the external electromagnetic field A^μ. The objective is to express the general invariant amplitude $\mathcal{M}$ in terms of different form factors. To achieve this, the Feynman diagram in Figure 1 is examined. The blob represents all possible higher-order loop corrections. The invariant amplitude can be written as $\mathcal{M} = \epsilon_\mu\mathcal{M}^\mu$, utilizing the polarization vector ϵ_μ. The following discussion is based on the literature [12, pp. 202–203] and [11, pp. 316–318].

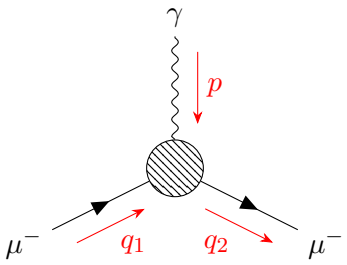

Figure 1: Interaction of the muon with an electromagnetic field. The blob represents all possible vertex corrections.

We start with a general approach, where $\mathcal{M}^\mu$ is a combination of all possible Lorentz vectors present in the blob. The Lorentz vectors are scaled by the functions f_i. These functions depend on possible Lorentz scalars, such as the scalar products $q_1 \cdot q_1$, $q_2 \cdot q_2$, and $q_1 \cdot q_2$. Since q_1 and q_2 are on-shell and $p^2 = 2m^2 - 2q_1 \cdot q_2$, the Lorentz factors f_i depend only on the kinematic variable p^2. Hence, the ensuing ansatz is adopted:

$$i\mathcal{M}^\mu = \bar{u}(q_2)\Big[f_1\gamma^\mu + f_2 p^\mu + f_3 Q^\mu + f_4\gamma^\mu\gamma_5 + f_5 p^\mu\gamma_5 + f_6 Q^\mu\gamma_5\Big]u(q_1). \tag{2.3.1}$$

Here we introduced $Q^\mu = q_1^\mu + q_2^\mu$, because due to the conservation of momentum $p^\mu = q_2^\mu - q_1^\mu$ there are only two independent momenta instead of three. The linear combination Q^μ is orthogonal to p^μ since the fermions are on-shell:

$$p \cdot Q = q_2^2 - q_1^2 = 0. \tag{2.3.2}$$

Additional constraints on the invariant amplitude imply that the coefficients f_i are interdependent.
An important condition is the Ward identity $p_\mu \mathcal{M}^\mu = 0$, which describes the fact that the photon has no longitudinal polarization and is necessary for a Lorentz-invariant theory. It thus applies:

$$\begin{aligned} ip_\mu\mathcal{M}^\mu =& p_\mu\bar{u}(q_2)\Big[f_1\gamma^\mu + f_2 p^\mu + f_3 Q^\mu \\ &+ f_4\gamma^\mu\gamma_5 + f_5 p^\mu\gamma_5 + f_6 Q^\mu\gamma_5\Big]u(q_1) \\ =& \bar{u}(q_2)\Big[f_1\not{p} + f_2 p^2 + f_3 p\cdot Q + f_4\not{p}\gamma_5 + f_5 p^2\gamma_5 + f_6 p\cdot Q\gamma_5\Big]u(q_1) \overset{!}{=} 0. \end{aligned} \tag{2.3.3}$$

Notice that the first term is zero because of the Dirac equation:

$$\begin{aligned} \bar{u}(q_2)\not{p}u(q_1) =& \bar{u}(q_2)[\not{q}_2 - \not{q}_1]u(q_1) \\ =& \bar{u}(q_2)[m - m]u(q_1) = 0. \end{aligned} \tag{2.3.4}$$

The term with the Lorentz scalar f_4 can be written as

$$\begin{aligned} \bar{u}(q_2)[f_4\not{p}\gamma_5]u(q_1) =& \bar{u}(q_2)[f_4(\not{q}_2 - \not{q}_1)\gamma_5]u(q_1) \\ =& \bar{u}(q_2)[f_4(\not{q}_2\gamma_5 + \gamma_5\not{q}_1)]u(q_1) \\ =& 2mf_4\bar{u}(q_2)\gamma_5 u(q_1). \end{aligned} \tag{2.3.5}$$

With $p \cdot Q = 0$, it can be derived that

$$ip_\mu\mathcal{M}^\mu = \bar{u}(q_2)\left[f_2 p^2 + 2mf_4\gamma_5 + f_5 p^2\gamma_5\right]u(q_1) = 0. \tag{2.3.6}$$

Since the identity $\mathbb{I}_4$ and γ_5 are linearly independent, each must individually be zero. Thus, it follows $f_2 = 0$ and

$$0 = f_4 2m + f_5 p^2$$
$$\Rightarrow f_5 = -\frac{f_4 2m}{p^2}.$$

Equation (2.3.1) can be expressed as

$$i\mathcal{M}^\mu = \bar{u}(q_2)\Big[f_1\gamma^\mu + f_3 Q^\mu + f_4\left(\gamma^\mu - \frac{2mp^\mu}{p^2}\right)\gamma_5 + f_6 Q^\mu\gamma_5\Big]u(q_1). \tag{2.3.7}$$

Employing the Gordon identities, results in

$$i\mathcal{M}^\mu = \bar{u}(q_2)\Big[f_1\gamma^\mu + f_3(2m\gamma^\mu - i\sigma^{\mu\nu}p_\nu) + f_4\left(\gamma^\mu - \frac{2mp^\mu}{p^2}\right)\gamma_5 - f_6 i\sigma^{\mu\nu}p_\nu\gamma_5\Big]u(q_1). \tag{2.3.8}$$

This expression can be characterized by four different form factors. Analogously to [12, p. 203], we define:

$$F_E = \frac{i}{e}(f_1 + 2mf_3), \qquad F_A = \frac{i}{e}f_4, \tag{2.3.9}$$
$$F_M = \frac{i}{e}(-f_3 2m), \qquad F_D = \frac{i}{e}(-i)f_6 2m, \tag{2.3.10}$$

with $F_E(p^2)$ as the electric charge form factor, $F_A(p^2)$ as the P violating anapole moment, $F_M(p^2)$ as the magnetic form factor and $F_D(p^2)$ as the CP violating electric dipole moment.
Now $i\mathcal{M}^\mu$, in terms of the form factors, can be written as:

$$i\mathcal{M}^\mu = (-ie)\bar{u}(q_2)\Big[F_E(p^2)\gamma^\mu + \left(\gamma^\mu - \frac{2mp^\mu}{p^2}\right)\gamma_5 F_A(p^2) + i\sigma^{\mu\nu}\frac{p_\nu}{2m}F_M(p^2) + \sigma^{\mu\nu}\frac{p_\nu}{2m}\gamma_5 F_D(p^2)\Big]u(q_1). \tag{2.3.11}$$

In QED, any terms involving γ_5 disappear because of the theory's parity invariance. With respect to the electric charge form factor, the condition $F_E(0) = 1$ holds as a result of the renormalization of charge. As demonstrated in the previous section, the gyromagnetic factor g is derived by multiplying $-4m/e$ with the coefficient of $i\sigma^{\mu\nu}\frac{p_\nu}{2m}$. Using the Gordon identity, this results in

$$g = 2\big(F_E(0) + F_M(0)\big) = 2\big(1 + F_M(0)\big). \tag{2.3.12}$$

The choice of $p^2 = 0$ arises from the classical limit, in which momentum transfer approaches zero.
If we compare the SM tree-level scenario with Equation (2.3.11), we observe $F_E(p^2) = 1$ and $F_i(p^2) = 0$ for $i = A, D, M$. It is therefore noteworthy that the electric charge form factor also describes the interaction via its magnetic moment. However, this alone leads to the expected factor $g = 2$ according to tree level. The anomalous magnetic moment is thus given by

$$a_\mu = \frac{g-2}{2} = F_M(0). \tag{2.3.13}$$

Due to radiation corrections for higher-order Feynman diagrams, a non-vanishing magnetic form factor is present and leads to an anomalous magnetic moment. Therefore, the objective is to extract the form factor F_M from the invariant amplitude $\mathcal{M}$. This is done in the next section for the largest occurring correction factor, the one-loop correction of QED.

2.4 One-Loop QED Contribution

The largest part of the anomalous magnetic moment a_μ is contributed by the corrections from QED. In this section, the dominant one-loop contribution to the Feynman diagram in Figure 2 is calculated.

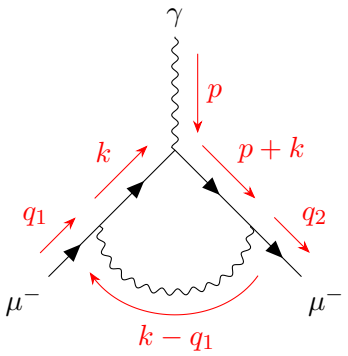

Figure 2: One-loop QED diagram that contributes to the AMM of the muon.

Although four momentum is conserved at each vertex, the momentum k is unrestricted. The possible magnitude of k is therefore given by $|k| \in [0, \infty)$. The integration $\int d^4k$ thus sums over all possible momentum values. Below, the dot representing the scalar product (using the Minkowski metric) between two four-momenta is dropped. Thus, expressions involving two momenta should be interpreted as scalar products. The following calculation is based on [11, pp. 318–320].

Using the Feynman rules, listed in Appendix A.6, the graph leads to $\mathcal{M} = \epsilon_\mu \mathcal{M}^\mu$ with

$$\begin{aligned} i\mathcal{M}^\mu = &\int \frac{d^4k}{(2\pi)^4} \bar{u}(q_2)(-ie\gamma^\nu) \frac{-ig_{\nu\alpha}}{(k-q_1)^2 + i\epsilon} \\ &\times \frac{i(\not{p} + \not{k} + m)}{(p+k)^2 - m^2 + i\epsilon}(-ie\gamma^\mu) \frac{i(\not{k} + m)}{k^2 - m^2 + i\epsilon}(-ie\gamma^\alpha) u(q_1) \\ = -e^3 \bar{u}(q_2) &\int \frac{d^4k}{(2\pi)^4} \frac{\gamma^\nu(\not{p} + \not{k} + m)\gamma^\mu(\not{k} + m)\gamma_\nu}{[(k-q_1)^2 + i\epsilon][(p+k)^2 - m^2 + i\epsilon][k^2 - m^2 + i\epsilon]} u(q_1). \end{aligned} \tag{2.4.1}$$

We will now closely examine $i\mathcal{M}^\mu$ and utilize the expression:

$$i\mathcal{M}^\mu = -e^3 \int \frac{d^4k}{(2\pi)^4} \frac{N^\mu}{ABC}. \tag{2.4.2}$$

In accordance with this, we define the following coefficients:

$$A = k^2 - m^2 + i\epsilon, \tag{2.4.3}$$

$$B = (p+k)^2 - m^2 + i\epsilon, \tag{2.4.4}$$

$$C = (k - q_1)^2 + i\epsilon. \tag{2.4.5}$$

Using the Feynman parametrization, the identity

$$\frac{1}{ABC} = 2\int dx\, dy\, dz\, \delta(x+y+z-1)\frac{1}{[xA+yB+zC]^3}, \tag{2.4.6}$$

demonstrated in Appendix A.7, can be implemented. In the following calculation, it is applied that

- the incoming and outgoing muon is on its mass shell:

$$q_1^2 = q_2^2 = m^2. \tag{2.4.7}$$

- four momentum conservation holds:

$$p^\mu = q_2^\mu - q_1^\mu. \tag{2.4.8}$$

- as a consequence of the δ-function in Eq. (2.4.6), the Feynman parameters must satisfy the condition:

$$x+y+z = 1. \tag{2.4.9}$$

The denominator of Eq. (2.4.1) can be expressed as the cube of

$$\begin{aligned}
xA+yB+zC &= x\big(k^2-m^2+i\epsilon\big) + y\big(p^2+2pk+k^2-m^2+i\epsilon\big) \\
&\quad + z\big(k^2-2kq_1+q_1^2+i\epsilon\big) \\
&= \big(k^2+i\epsilon\big)\big(x+y+z\big) - xm^2 + y\big(p^2+2pk-m^2\big) \\
&\quad + z\big(q_1^2-2kq_1\big) \\
&\overset{(2.4.9)}{=} k^2 - m^2(1-z) + y\big(p^2+2pk\big) + z\big(q_1^2-2kq_1\big) + i\epsilon \\
&\overset{(2.4.7)}{=} -m^2 + 2zm^2 - z^2m^2 + z^2m^2 + k^2 + y\big(p^2+2pk\big) \\
&\quad - 2zkq_1 + i\epsilon \\
&= -\big(1-z\big)^2m^2 + k^2 + z^2m^2 + 2ypk - 2zkq_1 \\
&\quad - 2yzpq_1 + 2yzpq_1 - y^2p^2 + y^2p^2 + yp^2 + i\epsilon \\
&\overset{(2.4.7,)}{=} -\big(1-z\big)^2m^2 + \big(k^\mu + yp^\mu - zq_1^\mu\big)^2 \\
&\quad + 2yzpq_1 - y^2p^2 + yp^2 + i\epsilon.
\end{aligned} \tag{2.4.10}$$

Here, zeros were added to enable factorization. With

$$pq_1 \overset{(2.4.8)}{=} \big(q_2-q_1\big)q_1 = \frac{1}{2}\big(2q_1q_2 - 2q_1^2\big) \overset{(2.4.7)}{=} -\frac{1}{2}\big(q_1^2+q_2^2-2q_2q_1\big) \overset{(2.4.8)}{=} -\frac{1}{2}p^2, \tag{2.4.11}$$

we derive

$$\begin{aligned}
xA+yB+zC &= \big(k^\mu + yp^\mu - zq_1^\mu\big)^2 + yp^2\big(1-y-z\big) - \big(1-z\big)^2m^2 + i\epsilon \\
&\overset{(2.4.9)}{=} \big(k^\mu + yp^\mu - zq_1^\mu\big)^2 - \Delta + i\epsilon,
\end{aligned} \tag{2.4.12}$$

where

$$\Delta \equiv -xyp^2 + \big(1-z\big)^2m^2 \tag{2.4.13}$$

is defined. After performing the substitution $k^\mu \to k^\mu - yp^\mu + zq_1^\mu$ and using the Feynman parametrization, Eq. (2.4.2) changes to

$$i\mathcal{M}^\mu = -2e^3 \int \frac{d^4k}{(2\pi)^4} \int_0^1 dx\, dy\, dz\, \delta(x+y+z-1) \frac{N'^\mu}{[k^2 - \Delta + i\epsilon]^3}. \tag{2.4.14}$$

Here, N'^μ denotes the shifted numerator. To proceed, we first transform the numerator before any substitution. Comparison of $i\mathcal{M}^\mu$ in Eq. (2.4.1) with the expression in Eq. (2.4.2) leads to

$$\begin{aligned} N^\mu &= \bar{u}(q_2)\Big[\gamma^\nu(\not{p} + \not{k} + m)\gamma^\mu(\not{k} + m)\gamma_\nu\Big]u(q_1) \\ &= \bar{u}(q_2)\Big[\gamma^\nu\not{p}\gamma^\mu\not{k}\gamma_\nu + \gamma^\nu\not{k}\gamma^\mu\not{k}\gamma_\nu + m\gamma^\nu\not{p}\gamma^\mu\gamma_\nu \\ &\qquad + m\gamma^\nu\not{k}\gamma^\mu\gamma_\nu + m\gamma^\nu\gamma^\mu\not{k}\gamma_\nu + m^2\gamma^\nu\gamma^\mu\gamma_\nu\Big]u(q_1). \end{aligned} \tag{2.4.15}$$

Using the identities for the gamma matrices in Appendix A.8, we observe that the first two terms can be rearranged as

$$\gamma^\nu \not{a}\gamma^\mu \not{b}\gamma_\nu = a_\alpha b_\beta \gamma^\nu\gamma^\alpha\gamma^\mu\gamma^\beta\gamma_\nu = -2a_\alpha b_\beta\gamma^\beta\gamma^\mu\gamma^\alpha = -2\not{b}\gamma^\mu\not{a}, \tag{2.4.16}$$

where $\not{a}$ and $\not{b}$ represent any Dirac slashed quantity. The terms linear in mass can be simplified to

$$\gamma^\nu\not{a}\gamma^\mu\gamma_\nu = a_\alpha\gamma^\nu\gamma^\alpha\gamma^\mu\gamma^\nu = 4a_\alpha g^{\alpha\mu} = 4a^\mu. \tag{2.4.17}$$

It is noteworthy that the last linear mass term in Eq. (2.4.15) has a different order of the two middle gamma matrices sandwiched by γ^ν and γ_ν. However, in Eq. (2.4.17), it is evident that due to the symmetric Minkowski matrix, we derive the same result.
The term quadratic in m already appears in the form of a gamma identity in the Appendix A.8. Plugging in the discussed terms yields

$$\begin{aligned} N^\mu &= \bar{u}(q_2)\Big[-2\not{k}\gamma^\mu\not{p} - 2\not{k}\gamma^\mu\not{k} - 2m^2\gamma^\mu + 8k^\mu m + 4p^\mu m\Big]u(q_1) \\ &= -2\bar{u}(q_2)\Big[\not{k}\gamma^\mu\not{p} + \not{k}\gamma^\mu\not{k} + m^2\gamma^\mu - 2m(p^\mu + 2k^\mu)\Big]u(q_1). \end{aligned} \tag{2.4.18}$$

The aforementioned substitution $k^\mu \to k^\mu - yp^\mu + zq_1^\mu$ leads to

$$\begin{aligned} -\frac{1}{2}N'^\mu = \bar{u}(q_2)\Big[&(\not{k} - y\not{p} + z\not{q}_1)\gamma^\mu\not{p} + (\not{k} - y\not{p} + z\not{q}_1)\gamma^\mu(\not{k} - y\not{p} + z\not{q}_1) \\ &+ m^2\gamma^\mu - 2m\Big(p^\mu + 2(k^\mu - yp^\mu + zq_1^\mu)\Big)\Big]u(q_1). \end{aligned} \tag{2.4.19}$$

We keep only the terms with even powers of k in the numerator, since the integrand will be antisymmetric under the transformation $k \to -k$ for terms with odd powers of k (discussed in Appendix A.9). This yields

$$\begin{aligned} -\frac{1}{2}N'^\mu &= \bar{u}(q_2)\Big[(-y\not{p} + z\not{q}_1)\gamma^\mu\not{p} + \not{k}\gamma^\mu\not{k} + (-y\not{p} + z\not{q}_1)\gamma^\mu(-y\not{p} + z\not{q}_1) \\ &\qquad + m^2\gamma^\mu - 2m\Big(p^\mu + 2(-yp^\mu + zq_1^\mu)\Big)\Big]u(q_1) \\ &= \bar{u}(q_2)\Big[\not{k}\gamma^\mu\not{k} + (-y\not{p} + z\not{q}_1)\gamma^\mu(\not{p} - y\not{p} + z\not{q}_1) \\ &\qquad + m^2\gamma^\mu - 2m(2zq_1^\mu - 2yp^\mu + p^\mu)\Big]u(q_1). \end{aligned} \tag{2.4.20}$$

Applying the Dirac equation along with the conservation of four-momentum $p^\mu = q_2^\mu - q_1^\mu$, results in:

$$\begin{aligned}
-\frac{1}{2}N'^\mu &= \bar{u}(q_2)\Big[\not{k}\gamma^\mu\not{k} + (-y\not{p} + z(m-\not{p}))\gamma^\mu(\not{p} - y\not{p} + zm) \\
&\qquad + m^2\gamma^\mu + 2m(2yp^\mu - 2zq_1^\mu - p^\mu)\Big]u(q_1) \\
&= \bar{u}(q_2)\Big[\not{k}\gamma^\mu\not{k} + ((-y-z)\not{p} + zm)\gamma^\mu((1-y)\not{p} + zm) \\
&\qquad + m^2\gamma^\mu + 2m(2yp^\mu - 2zq_1^\mu - p^\mu)\Big]u(q_1) \\
&\overset{(2.4.9)}{=} \bar{u}(q_2)\Big[\not{k}\gamma^\mu\not{k} - (1-x)(1-y)\not{p}\gamma^\mu\not{p} + zm(1-y)\gamma^\mu\not{p} - zm(1-x)\not{p}\gamma^\mu \\
&\qquad + z^2m^2\gamma^\mu + m^2\gamma^\mu + 2m\Big((2y-1)p^\mu - 2zq_1^\mu\Big)\Big]u(q_1). \qquad (2.4.21)
\end{aligned}$$

At this point, it makes sense to think of the form factors in Section 2.3. Since we calculate a (parity invariant) QED correction, the invariant amplitude $i\mathcal{M}$ can be expressed via the electric charge form factor F_E and the magnetic form factor F_M. To achieve this, the terms must initially be transformed into a form that relies solely on a single Lorentz vector. This transformation utilizes the gamma matrix identities presented in Appendix A.8:

$$\begin{aligned}
\bar{u}(q_2)\Big[\not{k}\gamma^\mu\not{k}\Big]u(q_1) &= \bar{u}(q_2)[k_\alpha k_\beta\gamma^\alpha\gamma^\mu\gamma^\beta]u(q_1) \\
&\overset{(A.9)}{=} \bar{u}(q_2)\Big[\frac{1}{4}g_{\alpha\beta}k^2\gamma^\alpha\gamma^\mu\gamma^\beta\Big]u(q_1) \\
&= \bar{u}(q_2)\Big[-\frac{1}{2}k^2\gamma^\mu\Big]u(q_1), \qquad (2.4.22) \\
\bar{u}(q_2)[\not{p}\gamma^\mu\not{p}]u(q_2) &= \bar{u}(q_2)[p_\alpha p_\beta\gamma^\alpha\gamma^\mu\gamma^\beta]u(q_1) \\
&= \bar{u}(q_2)[p_\alpha p_\beta\gamma^\alpha(2g^{\mu\beta} - \gamma^\beta\gamma^\mu)]u(q_1) \\
&= \bar{u}(q_2)[2p^\mu\not{p} - \not{p}\not{p}\gamma^\mu]u(q_1) \\
&\overset{*}{=} \bar{u}(q_2)[2p^\mu\not{p} - p^2\gamma^\mu]u(q_1) \\
&\overset{(2.4.7)}{=} \bar{u}(q_2)[-p^2\gamma^\mu]u(q_1), \qquad (2.4.23) \\
\bar{u}(q_2)[\gamma^\mu\not{p}]u(q_1) &= \bar{u}(q_2)[\gamma^\mu(\not{q}_2 - \not{q}_1)]u(q_1) \\
&\overset{(2.4.7)}{=} \bar{u}(q_2)[\gamma^\mu(q_{2\alpha}\gamma^\alpha - m)]u(q_1) \\
&= \bar{u}(q_2)[q_{2\alpha}(2g^{\mu\alpha} - \gamma^\alpha\gamma^\mu) - m\gamma^\mu]u(q_1) \\
&= \bar{u}(q_2)[2q_2^\mu - \not{q}_2\gamma^\mu - m\gamma^\mu]u(q_1) \\
&\overset{(2.4.7)}{=} 2\bar{u}(q_2)[q_2^\mu - m\gamma^\mu]u(q_1), \qquad (2.4.24) \\
\bar{u}(q_2)[\not{p}\gamma^\mu]u(q_1) &\overset{(2.4.8)}{=} 2\bar{u}(q_2)[m\gamma^\mu - q_1^\mu]u(q_1). \qquad (2.4.25)
\end{aligned}$$

Equation (2.4.25) was derived analogously to identity (2.4.24). In Eq. (2.4.23) the marked step ($\overset{*}{=}$) can be shown using the anticommutator relation:

$$\not{p}\not{p} = p_\alpha p_\beta\gamma^\alpha\gamma^\beta = 2p^2 - \not{p}\not{p} \qquad \Rightarrow \qquad \not{p}\not{p} = p^2.$$

Applying the identities illustrated above results in

$$-\frac{1}{2}N'^\mu = \bar{u}(q_2)\Big[-\frac{1}{2}k^2\gamma^\mu + (1-x)(1-y)p^2\gamma^\mu + 2z(1-y)m(q_2^\mu - m\gamma^\mu)$$

$$
\begin{aligned}
&- 2z(1-x)m(m\gamma^\mu - q_1^\mu) + z^2m^2\gamma^\mu + m^2\gamma^\mu \\
&+ 2m\Big((2y-1)p^\mu - 2zq_1^\mu\Big)\Big]u(q_1). \qquad (2.4.26)
\end{aligned}
$$

Sorting the expressions according to the four Lorentz vectors yields

$$
\begin{aligned}
-\frac{1}{2}N'^\mu = \bar{u}(q_2)\Big[\Big(-\frac{1}{2}k^2 + (1-x)(1-y)p^2 + z^2m^2 + m^2 - 2zm^2(2-x-y)\Big)\gamma^\mu \\
\underbrace{+2(2y-1)mp^\mu + (2zm(1-x) - 4zm)q_1^\mu + 2z(1-y)mq_2^\mu}_{\equiv\xi^\mu}\Big]u(q_1). \qquad (2.4.27)
\end{aligned}
$$

It is observed that the γ^μ term contributes to the form factor F_E due to renormalization; this factor leads to $g = 2$ and is irrelevant for the anomalous magnetic behavior. To apply the Gordon identity and thus infer the anomalous magnetic moment, we rearrange ξ^μ into the form

$$
\xi^\mu = a(q_2^\mu - q_1^\mu) + b(q_1^\mu + q_2^\mu), \qquad (2.4.28)
$$

where a and b are Lorentz scalar coefficients. We can split ξ^μ into a term dependent on q_1^μ and q_2^μ:

$$
\begin{aligned}
\xi^\mu &= 2(2y-1)mp^\mu + (2zm(1-x) - 4zm)q_1^\mu + 2z(1-y)mq_2^\mu \\
&\overset{(2.4.8),(2.4.9)}{=} 2m(2y-1)(q_2^\mu - q_1^\mu) + 2z(y+z-2)mq_1^\mu + 2z(1-y)mq_2^\mu \\
&= \underbrace{2m\Big(2y-1+z(1-y)\Big)}_{\text{(I)}}q_2^\mu + \underbrace{2m\Big(z(y+z-2) - (2y-1)\Big)}_{\text{(II)}}q_1^\mu. \qquad (2.4.29)
\end{aligned}
$$

The coefficients a and b in Eq. (2.4.28) are determined by

$$
a = \frac{\text{(I)} - \text{(II)}}{2} \qquad \text{and} \qquad b = \frac{\text{(I)} + \text{(II)}}{2}. \qquad (2.4.30)
$$

Hence, we obtain the coefficients

$$
\begin{aligned}
a &= \big[4y - 2 + z(1-2y-z+2)\big]m \\
&\overset{(2.4.9)}{=} \big[4y - 2 + 3z - 2yz - z(1-x-y)\big]m \\
&\overset{(2.4.9)}{=} \big[4y - 2(x+y+z) + 2z - yz + xz\big]m \\
&= \big[2y - 2x - yz + xz\big]m \\
&= (z-2)(x-y)m \qquad (2.4.31)
\end{aligned}
$$

and

$$
\begin{aligned}
b =& \big[2y - 1 + z(1-y) + z(y+z-2) - (2y-1)\big]m \\
=& z(z-1)m. \qquad (2.4.32)
\end{aligned}
$$

Therefore, it follows

$$
\xi^\mu = (z-2)(x-y)mp^\mu + z(z-1)m(q_1^\mu + q_2^\mu). \qquad (2.4.33)
$$

Using the Gordon identity, yields

$$\bar{u}(q_2)\xi^\mu u(q_1) = \bar{u}(q_2)\Big[(z-2)(x-y)mp^\mu + 2z(z-1)m^2\gamma^\mu - iz(z-1)m\sigma^{\mu\nu}p_\nu\Big]u(q_1). \tag{2.4.34}$$

The numerator can then be expressed as

$$\begin{aligned}
-\frac{1}{2}N'^\mu &= \bar{u}(q_2)\Big[\Big(-\frac{1}{2}k^2 + (1-x)(1-y)p^2 + z^2m^2 + m^2 - 2zm^2(2-x-y)\Big)\gamma^\mu \\
&\qquad + (z-2)(x-y)mp^\mu + 2z(z-1)m^2\gamma^\mu - iz(z-1)m\sigma^{\mu\nu}p_\nu\Big]u(q_1) \\
&\overset{(2.4.9)}{=} \bar{u}(q_2)\Big[\Big(-\frac{1}{2}k^2 + (1-x)(1-y)p^2 + z^2m^2 + m^2 - 4zm^2\Big)\gamma^\mu \\
&\qquad + (z-2)(x-y)mp^\mu + iz(1-z)m\sigma^{\mu\nu}p_\nu\Big]u(q_1) \\
&= \Big(-\frac{1}{2}k^2 + (1-x)(1-y)p^2 + (1-4z+z^2)m^2\Big)\bar{u}(q_2)\gamma^\mu u(q_1) \\
&\qquad + iz(1-z)mp_\nu\bar{u}(q_2)\sigma^{\mu\nu}u(q_1) + (z-2)(x-y)p^\mu\bar{u}(q_2)u(q_1).
\end{aligned} \tag{2.4.35}$$

We have three independent terms instead of two like expected in QED. By applying the Ward identity $p_\mu\mathcal{M}^\mu = 0$, it becomes clear that the term proportional to p^μ must disappear.[1] This becomes evident in the computation because of the integration of the form

$$\int_0^1 dx\,dy\,dz\,\delta(x+y+z)(z-2)(x-y)\int\frac{d^4k}{(2\pi)^4}\frac{p^\mu}{(k^2-\Delta+i\epsilon)^3}\bar{u}(q_2)u(q_1). \tag{2.4.36}$$

In the exchange $x \leftrightarrow y$, both the δ-function and the defined Δ are symmetric. However, the integrand is antisymmetric under this exchange, making the integral zero.
To determine the magnetic form factor F_M, we need to compare the $p_\nu\sigma^{\mu\nu}$ term with Eq. (2.3.11), leading to

$$F_M = \frac{2m}{e}(4ie^3m)\int_0^1 dx\,dy\,dz\,\delta(x+y+z-1)\int\frac{d^4k}{(2\pi)^4}\,\frac{z(1-z)}{(k^2-\Delta+i\epsilon)^3}. \tag{2.4.37}$$

The integration over momentum can be executed by transforming to the Euclidean metric through a process known as Wick rotation, which is illustrated in Appendix A.10:

$$\int\frac{d^4k}{(2\pi)^4}\frac{1}{(k^2-\Delta+i\epsilon)^3} = \frac{-i}{32\pi^2\Delta}. \tag{2.4.38}$$

With $\alpha = e^2/(4\pi)$, this leads to

$$F_M(p^2) = \frac{\alpha}{\pi}m^2\int_0^1 dx\,dy\,dz\,\delta(x+y+z-1)\frac{z(1-z)}{(1-z)^2m^2 - xyp^2}. \tag{2.4.39}$$

As discussed in Section 2.3, the anomalous magnetic moment is given by $a_\mu = F_M(0)$. We can carry out the integration, which yields

$$F_M(0) = \frac{\alpha}{\pi}\int_0^1 dz\int_0^1 dy\int_0^1 dx\,\delta(x+y+z-1)\frac{z}{1-z}$$

[1] This arises because the γ^μ term cancels out as a result of the Dirac equation, and the $p_\nu\sigma^{\mu\nu}$ term, being a product of symmetric and antisymmetric components under index interchange, also disappears.

$$
\begin{aligned}
&= \frac{\pi}{\alpha} \int_0^1 dz \int_0^{1-z} dy \, \frac{z}{1-z} \\
&= \frac{\alpha}{\pi} \int_0^1 dz \, z \\
&= \frac{\alpha}{2\pi}.
\end{aligned} \tag{2.4.40}
$$

The limits of the y-integration after applying the δ-function are given by

$$
\begin{aligned}
0 \leq x = 1 - (y+z) \leq 1 \qquad &\Leftrightarrow \qquad -1 \leq -(y+z) \leq 0 \\
&\Leftrightarrow \qquad -z \leq y \leq 1 - z.
\end{aligned}
$$

The lower limit does not offer any further restriction since $-z \leq 0$ is valid. The limits of integration are therefore determined by $0 \leq y \leq 1 - z$.

Thus, it was shown that the one-loop QED correction leads to

$$
a_\mu = \frac{\alpha}{2\pi} \approx 0.00116 \qquad \text{resp.} \qquad g = 2\left(1 + \frac{\alpha}{2\pi}\right) \approx 2.00232.
$$

The result was first calculated by Julian Schwinger in 1948 [13]. As we can see, our result is independent of the muon mass, so the electron and tau have the same QED one-loop contribution.

In general, loop corrections incorporate lepton-specific effects due to their mass dependencies. Examining higher-order QED corrections results in a series expansion in terms of the coupling constants α. In addition to the dominant QED corrections, there are electroweak and hadronic contributions. The electroweak one-loop contribution is made up of three diagrams. Two of them contain a vector boson (W or Z boson), while the third is based on the scalar Higgs boson H. The hadronic contributions are the primary source of uncertainty in the muon's AMM. Due to their non-perturbative nature, one potential calculation method is lattice QCD.

3 One-Loop Contributions for Scalar-Fermion Interactions

The discrepancy between the SM value and the experimental value of the AMM has led to investigations into physics BSM. We aim to introduce BSM particles that interact with SM particles. This approach is worthwhile because parameters such as the masses of BSM particles are often not fixed by current data. We examine the one-loop weak correction of the AMM with respect to internal scalar and fermion lines.
Within the framework of Lorentz invariance and U(1) gauge invariance in QED, three contributions can be identified. Apart from the case where a scalar H couples with a fermion F, which is discussed in the subsequent sections, there are scenarios involving loops with fermions F and vector bosons V, or loops with fermions F, vector bosons V and scalars H that contribute to the AMM [14].
The relevant interaction Lagrangian after spontaneous symmetry breaking is given by [14]:

$$
\mathcal{L}_{\text{int}}^{\text{FH}} = \sum_{F,H} \Big[\overline{[\mu^-}(C_S + C_P\gamma^5)FH + \text{H.c.}] + Q_F e \overline{F} \gamma_\mu A^\mu F + i Q_H e \big(H^* \partial_\mu H - H \partial_\mu H^*\big) A^\mu \Big]. \tag{3.0.1}
$$

With the Hermitian conjugate:

$$\begin{aligned}\text{H.c.} &= \left[\overline{\mu^-}(C_S + C_P\gamma^5)FH\right]^\dagger \\ &= \left[H^*F^\dagger(C_S^* + C_P^*\gamma^5)\overline{\mu^-}^\dagger\right] \\ &= \left[H^*F^\dagger(C_S^* + C_P^*\gamma^5)\gamma^0\mu^-\right] \\ &= \left[H^*\overline{F}(C_S^* - C_P^*\gamma^5)\mu^-\right]. \end{aligned} \tag{3.0.2}$$

Here, C_S and C_P are scalar and pseudoscalar coupling constants, respectively. These constants are model dependent and can be derived from the corresponding Lagrangian. The introduced sum covers all fermions F and scalars H in the theory under consideration. The new vertex factors can be determined from the Lagrangians and the associated quantum fields. They are given by:

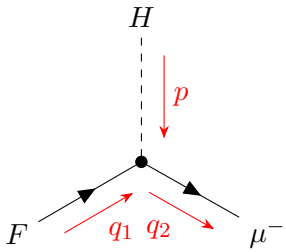

$= i(C_S + C_P\gamma^5),$

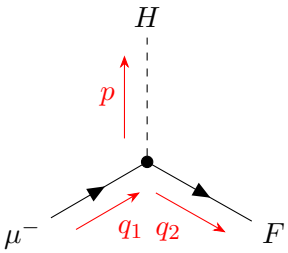

$= i(C_S^* - C_P^*\gamma^5)$

and

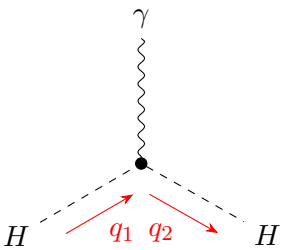

$= iQ_H(q_1 + q_2)^\mu.$

For the fermion-scalar vertex, this can be shown analogue to the QED vertex in Eq. (2.2.13). In the case of the scalar-photon vertex, the derivatives lead to a momentum dependence. This becomes clear through:

$$\begin{aligned} &iQ_H e \int d^4x \, \langle 0|a_{q_2}(H^*\partial^\mu H - H\partial^\mu H^*)A_\mu a^\dagger_{q_1} a_p^{\lambda\dagger}|0\rangle \prod_{i=q_1,q_2,p} \sqrt{2E_i} \\ =&iQ_H e \int dx^4 \, \langle 0|\Big(e^{iq_2\cdot x}(-iq_1^\mu)e^{-iq_1\cdot x} - e^{-iq_1\cdot x}(iq_2^\mu)e^{iq_2\cdot x}\Big)\epsilon_\mu e^{-ip\cdot x}|0\rangle \\ =&(2\pi)^4\delta^{(4)}(p + q_1 - q_2)\underbrace{Q_H e(q_1 + q_2)^\mu\epsilon_\mu}_{\overset{!}{=}\epsilon_\mu\mathcal{M}^\mu}. \end{aligned} \tag{3.0.3}$$

The possible Feynman diagrams are shown in Figure 3. In both cases, we observe the condition $Q_F + Q_H = -1$ due to the conservation of electric charge. The respective particle in the graph that couples to the electromagnetic field A^μ must be minimally singly charged.

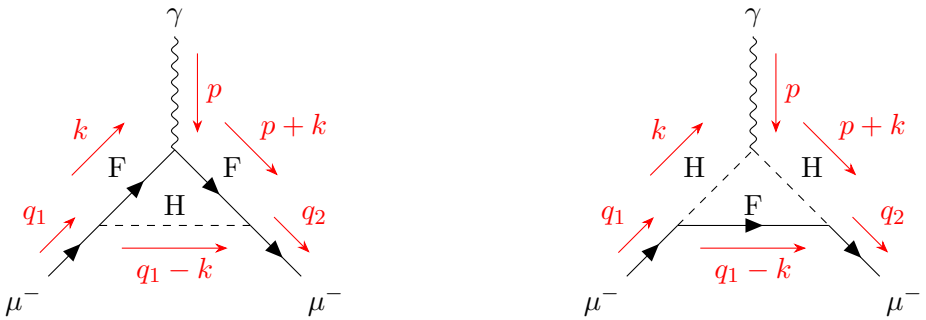

Figure 3: The two possible one-loop Feynman diagrams, including both fermions and scalars.

3.1 Photoemission from the Internal Fermion Line

In the following, the contribution to the AMM a_μ from diagram 3a is derived from the corresponding invariant amplitude $\mathcal{M} = \epsilon_\mu \mathcal{M}^\mu$. In contrast, the result of the topology 3b is given later. Using the Feynman rules, we derive

$$\begin{aligned} i\mathcal{M}^\mu = &\int \frac{d^4k}{(2\pi)^4} \frac{i}{(q_1-k)^2 - m_H^2 + i\epsilon} \bar{u}(q_2) i(C_S + C_P\gamma^5) \\ &\times \frac{i(\not{p} + \not{k} + m_F)}{(p+k)^2 - m_F^2 + i\epsilon} (ieQ_F\gamma^\mu) \frac{i(\not{k} + m_F)}{k^2 - m_F^2 + i\epsilon} i(C_S^* - C_P^*\gamma^5) u(q_1) \\ = -eQ_F\bar{u}(q_2) &\int \frac{d^4k}{(2\pi)^4} \frac{(C_S + C_P\gamma^5)(\not{p} + \not{k} + m_F)\gamma^\mu(\not{k} + m_F)(C_S^* - C_P^*\gamma^5)}{[(k-q_1)^2 - m_H^2 + i\epsilon][(p+k)^2 - m_F^2 + i\epsilon][k^2 - m_F^2 + i\epsilon]} u(q_1). \end{aligned} \tag{3.1.1}$$

The calculation will be structure-analogous to the standard model calculation in Section 2.4. Again, we use the expression:

$$i\mathcal{M}^\mu = -eQ_F \int \frac{d^4k}{(2\pi)^4} \frac{N^\mu}{ABC}. \tag{3.1.2}$$

The factors of the denominator can be defined as

$$A = k^2 - m_F^2 + i\epsilon, \tag{3.1.3}$$
$$B = (p+k)^2 - m_F^2 + i\epsilon, \tag{3.1.4}$$
$$C = (k-q_1)^2 - m_H^2 + i\epsilon. \tag{3.1.5}$$

A similar calculation to that in Sec. 2.4 can be carried out by incorporating the Feynman parameters, resulting in differences due to the varying masses of the internal and external legs:

$$\begin{aligned} xA + yB + zC &= x(k^2 - m_F^2 + i\epsilon) + y(p^2 + 2pk + k^2 - m_F^2 + i\epsilon) \\ &\quad + z(k^2 - 2kq_1 + q_1^2 - m_H^2 + i\epsilon) \\ &\overset{(2.4.9)}{=} k^2 - m_F^2(1-z) + y(p^2 + 2pk) + z(q_1^2 - 2kq_1 - m_H^2) + i\epsilon \\ &\overset{(2.4.7)}{=} -(1-z)m_F^2 - z^2 m_\mu^2 + z^2 m_\mu^2 + k^2 + y(p^2 + 2pk) \end{aligned}$$

$$
\begin{aligned}
&\quad + z(m_\mu^2 - 2kq_1 - m_H^2) + i\epsilon \\
&= -(1-z)m_F^2 - (z^2-z)m_\mu^2 + k^2 + z^2 m_\mu^2 + 2ypk \\
&\quad - 2zkq_1 - 2yzpq_1 + 2yzpq_1 + y^2p^2 - y^2p^2 + yp^2 - zm_H^2 + i\epsilon \\
&\overset{(2.4.7)}{=} -(1-z)m_F^2 - (z^2-z)m_\mu^2 - zm_H^2 + \left(k^\mu + yp^\mu - zq_1^\mu\right)^2 \\
&\quad + \underbrace{2yzpq_1 - y^2p^2 + yp^2}_{\overset{(2.4.11)}{=} y(1-z-y)p^2 \overset{(2.4.9)}{=} xyp^2} + i\epsilon.
\end{aligned} \tag{3.1.6}
$$

This results in

$$
xA + yB + zC = \left(k^\mu + yp^\mu - zq_1^\mu\right)^2 - \Delta + i\epsilon, \tag{3.1.7}
$$

with a slightly different definition

$$
\Delta \equiv -xyp^2 + (1-z)m_F^2 + (z^2-z)m_\mu^2 + zm_H^2 \tag{3.1.8}
$$

compared to Eq. (2.4.13). After the substitution $k^\mu \to k^\mu - yp^\mu + zq_1^\mu$, we obtain the form

$$
i\mathcal{M}^\mu = -2eQ_F \int \frac{d^4k}{(2\pi)^4} \int dx\, dy\, dz\, \delta(x+y+z-1) \frac{N'^\mu}{[k^2 - \Delta + i\epsilon]^3} \tag{3.1.9}
$$

with the numerator N'^μ, shifted by the substitution. The numerator can be rearranged as

$$
\begin{aligned}
N'^\mu &= \bar{u}(q_2)(C_S + C_P\gamma^5)(\not{p} + \not{k} - y\not{p} + z\not{q}_1 + m_F)\gamma^\mu \\
&\qquad \times (\not{k} - y\not{p} + z\not{q}_1 + m_F)(C_S^* - C_P^*\gamma^5)u(q_1) \\
&= \bar{u}(q_2)(C_S + C_P\gamma^5)\Big[\not{k}\gamma^\mu\not{k} + \not{k}\gamma^\mu(-y\not{p} + z\not{q}_1 + m_F) \\
&\qquad + ((1-y)\not{p} + z\not{q}_1 + m_F)\gamma^\mu\not{k} \\
&\qquad + ((1-y)\not{p} + z\not{q}_1 + m_F)\gamma^\mu(-y\not{p} + z\not{q}_1 + m_F)\Big](C_S^* - C_P^*\gamma^5)u(q_1).
\end{aligned} \tag{3.1.10}
$$

As explained in Appendix A.9, the linear terms in k vanish. With momentum conservation $p^\mu = q_2^\mu - q_1^\mu$, the shifted numerator becomes

$$
\begin{aligned}
N'^\mu &= \bar{u}(q_2)(C_S + C_P\gamma^5)\Big[\not{k}\gamma^\mu\not{k} \\
&\qquad + ((1-y)\not{p} + z(\not{q}_2 - \not{p}) + m_F)\gamma^\mu(-y\not{p} + z\not{q}_1 + m_F)\Big](C_S^* - C_P^*\gamma^5)u(q_1) \\
&\overset{(2.4.9)}{=} \bar{u}(q_2)(C_S + C_P\gamma^5)\Big[\not{k}\gamma^\mu\not{k} \\
&\qquad + (x\not{p} + z\not{q}_2 + m_F)\gamma^\mu(-y\not{p} + z\not{q}_1 + m_F)\Big](C_S^* - C_P^*\gamma^5)u(q_1) \\
&= \bar{u}(q_2)(C_S + C_P\gamma^5)\Big[\underbrace{\not{k}\gamma^\mu\not{k} + (x\not{p} + z\not{q}_2)\gamma^\mu(-y\not{p} + z\not{q}_1) + m_F^2\gamma^\mu}_{\equiv T^\mu_{\text{odd}}} \\
&\qquad \underbrace{+ m_F\gamma^\mu(-y\not{p} + z\not{q}_1) + m_F(x\not{p} + z\not{q}_2)\gamma^\mu}_{\equiv T^\mu_{\text{even}}}\Big](C_S^* - C_P^*\gamma^5)u(q_1).
\end{aligned} \tag{3.1.11}
$$

The expressions labeled as T^μ_{odd} represent combinations involving an odd count of gamma matrices, while those labeled as T^μ_{even} denote combinations involving an even count of gamma matrices. Due to the identities of the matrix γ^5, we can utilize

$$
\gamma^\mu\gamma^\nu\gamma^\rho = -\gamma^5\gamma^\mu\gamma^\nu\gamma^\rho\gamma^5, \qquad \gamma^5\gamma^\mu\gamma^\nu\gamma^\rho = -\gamma^\mu\gamma^\nu\gamma^\rho\gamma^5 \tag{3.1.12}
$$

and

$$\gamma^\mu\gamma^\nu = \gamma^5\gamma^\mu\gamma^\nu\gamma^5, \qquad \gamma^5\gamma^\mu\gamma^\nu = \gamma^\mu\gamma^\nu\gamma^5. \tag{3.1.13}$$

Using the relations (3.1.12) together with the Dirac equation allows the term, which contains an odd number of gamma matrices, to be reexpressed as follows:

$$\begin{aligned}
&\bar{u}(q_2)(C_S + C_P\gamma^5)T^\mu_{\text{odd}}(C_S^* - C_P^*\gamma^5)u(q_1)\\
=\;& \bar{u}(q_2)\Big[\Big(-\frac{1}{2}k^2\gamma^\mu + xyp^2\gamma^\mu + xz2m_\mu(m_\mu\gamma^\mu - q_1^\mu) - yz2m_\mu(q_2^\mu - m_\mu\gamma^\mu)\\
&\qquad + z^2m_\mu^2\gamma^\mu + m_F^2\gamma^\mu\Big)(|C_S|^2 + |C_P|^2) + M^\mu_{\text{odd}}\Big]u(q_1)\\
\overset{(2.4.9)}{=}\;& \bar{u}(q_2)\Big[\Big((-\frac{1}{2}k^2 + xyp^2 + z(2-z)m_\mu^2 + m_F^2)\gamma^\mu\\
&\qquad + 2m_\mu(-xzq_1^\mu - yzq_2^\mu)\Big)(|C_S|^2 + |C_P|^2) + M^\mu_{\text{odd}}\Big]u(q_1).
\end{aligned} \tag{3.1.14}$$

Nevertheless, the mixed terms in C_S and C_P, denoted as M^μ_{odd}, were not evaluated in this context because they require new identities that were not established in Section 2.4. For completeness, the mixed terms in C_S and C_P are still considered, even though they cannot contribute to the magnetic moment due to their proportionality to γ^5. Using the relations (3.1.13), we can analogously simplify the terms involving two gamma matrices:

$$\begin{aligned}
&\bar{u}(q_2)(C_S + C_P\gamma^5)T^\mu_{\text{even}}(C_S^* - C_P^*\gamma^5)u(q_1)\\
=\;& \bar{u}(q_2)\Big[\Big(-2ym_F(q_2^\mu - m_\mu\gamma^\mu) + zm_Fm_\mu\gamma^\mu + 2xm_F(m_\mu\gamma^\mu - q_1^\mu)\\
&\qquad + zm_Fm_\mu\gamma^\mu\Big)(|C_S|^2 - |C_P|^2) + M^\mu_{\text{even}}\Big]u(q_1)\\
\overset{(2.4.9)}{=}\;& \bar{u}(q_2)\Big[\Big(2m_Fm_\mu\gamma^\mu + 2m_F(-yq_2^\mu - xq_1^\mu)\Big)(|C_S|^2 - |C_P|^2) + M^\mu_{\text{even}}\Big]u(q_1).
\end{aligned} \tag{3.1.15}$$

Here, M^μ_{even} contains the mixed terms in C_S and C_P. For M^μ_{odd}, the following identities are required:

$$\begin{aligned}
\bar{u}(q_2)[\gamma^5\not{k}\gamma^\mu\not{k}]u(q_1) &\overset{(2.4.22)}{=} \bar{u}(q_2)\left[-\frac{1}{2}k^2\gamma^5\gamma^\mu\right]u(q_1)\\
&= \bar{u}(q_2)\left[\frac{1}{2}k^2\gamma^\mu\gamma^5\right]u(q_1),
\end{aligned} \tag{3.1.16}$$

$$\begin{aligned}
\bar{u}(q_2)[\gamma^5\not{p}\gamma^\mu\not{p}]u(q_1) &\overset{(2.4.23)}{=} \bar{u}(q_2)[\gamma^5(2p^\mu\not{p} - p^2\gamma^\mu)]u(q_1)\\
&= \bar{u}(q_2)[2p^\mu((-\not{q}_2)\gamma^5 - \gamma^5\not{q}_1) + p^2\gamma^\mu\gamma^5]u(q_1)\\
&\overset{(2.4.7)}{=} \bar{u}(q_2)[-4m_\mu p^\mu\gamma^5 + p^2\gamma^\mu\gamma^5]u(q_1),
\end{aligned} \tag{3.1.17}$$

$$\begin{aligned}
\bar{u}(q_2)[\gamma^5\not{q}_2\gamma^\mu\not{q}_1]u(q_1) &= \bar{u}(q_2)[-\not{q}_2\gamma^5\gamma^\mu\not{q}_1]u(q_1)\\
&\overset{(2.4.7)}{=} \bar{u}(q_2)[m_\mu^2\gamma^\mu\gamma^5]u(q_1),
\end{aligned} \tag{3.1.18}$$

$$\begin{aligned}
\bar{u}(q_2)[\gamma^5\not{q}_2\gamma^\mu\not{p}]u(q_1) &\overset{(2.4.7)}{=} \bar{u}(q_2)[-m_\mu\gamma^5\gamma^\mu\not{p}]u(q_1)\\
&\overset{(2.4.24)}{=} \bar{u}(q_2)[-m_\mu\gamma^5(2q_2^\mu - \not{q}_2\gamma^\mu - m_\mu\gamma^\mu)]u(q_1)\\
&\overset{(2.4.7)}{=} \bar{u}(q_2)[-m_\mu(2q_2^\mu\gamma^\mu - m_\mu\gamma^\mu\gamma^5 + m_\mu\gamma^\mu\gamma^5)]u(q_1)
\end{aligned}$$

$$= \bar{u}(q_2)\big[-2m_\mu q_2^\mu \gamma^5\big]u(q_1), \tag{3.1.19}$$

$$\bar{u}(q_2)\big[\gamma^5 \not{p}\gamma^\mu \not{q}_1\big]u(q_1) = \bar{u}(q_2)\big[-2m_\mu q_1^\mu \gamma^5\big]u(q_1). \tag{3.1.20}$$

For the terms labeled M^μ_{even} in Eq. (3.1.15), the subsequent identities are necessary:

$$\begin{aligned}\bar{u}(q_2)\big[\gamma^\mu \not{p}\gamma^5\big]u(q_1) &\overset{(2.4.24)}{=} \bar{u}(q_2)\big[\gamma_5(2q_2^\mu - \not{q}_2\gamma^\mu - \not{q}_1\gamma^\mu)\big]u(q_1)\\ &= \bar{u}(q_2)\big[2q_2^\mu\gamma^5\big]u(q_1),\end{aligned} \tag{3.1.21}$$

$$\bar{u}(q_2)\big[\not{p}\gamma^\mu\gamma^5\big]u(q_1) = \bar{u}(q_2)\big[-2q_1^\mu\gamma^5\big]u(q_1), \tag{3.1.22}$$

$$\bar{u}(q_2)\big[\gamma^\mu \not{q}_1\gamma^5\big]u(q_1) = \bar{u}(q_2)\big[-\not{q}_2\gamma^\mu\gamma^5\big]u(q_1). \tag{3.1.23}$$

The unified result for both mixed terms considered is given by

$$\begin{aligned}&\bar{u}(q_2)\big[M^\mu_{\text{odd}} + M^\mu_{\text{even}}\big]u(q_1)\\
&= \bar{u}(q_2)\Big[2\,\mathrm{Re}\,(C_S C_P^*)\Big(\frac{1}{2}k^2\gamma^\mu + xy(4m_\mu p^\mu - p^2\gamma^\mu) + z^2m_\mu^2\gamma^\mu - 2xzm_\mu q_1^\mu\\
&\qquad + 2yzm_\mu q_2^\mu - 2m_F^2\gamma^\mu\Big) + 2i\,\mathrm{Im}(C_S C_P^*)2m_F(xq_1^\mu + yq_2^\mu)\Big]\gamma^5 u(q_1)\\
&\overset{(2.4.8)}{=} \bar{u}(q_2)\,\mathrm{Re}(C_S C_P^*)\Big[\Big((k^2 - 2xyp^2 + 2z^2m_\mu^2 - 2m_F^2)\gamma^\mu + (4yzm_\mu + 8xym_\mu)q_2^\mu\\
&\qquad - (4xzm_\mu + 8xym_\mu)q_1^\mu\Big) + i\,\mathrm{Im}\,(C_S C_P^*)4m_F(xq_1^\mu + yq_2^\mu)\Big]\gamma^5 u(q_1)\\
&= \bar{u}(q_2)\Big[\mathrm{Re}(C_S C_P^*)\Big((k^2 - 2xyp^2 + 2z^2m_\mu^2 - 2m_F^2)\gamma^\mu + 4y(z+2x)m_\mu q_2^\mu\\
&\qquad - 4x(z+2y)m_\mu q_1^\mu\Big) + i\,\mathrm{Im}\,(C_S C_P^*)4m_F(xq_1^\mu + yq_2^\mu)\Big]\gamma^5 u(q_1).\end{aligned} \tag{3.1.24}$$

Plugging all together the numerator N'^μ results in

$$\begin{aligned}N'^\mu = \bar{u}(q_2)\Big[&\underbrace{\Big(-2yzm_\mu(|C_S|^2 + |C_P|^2) - 2ym_F(|C_S|^2 - |C_P|^2)\Big)}_{(\mathrm{I})_\alpha} q_2^\mu\\
&+ \underbrace{\Big(-2xzm_\mu(|C_S|^2 + |C_P|^2) - 2xm_F(|C_S|^2 - |C_P|^2)\Big)}_{(\mathrm{II})_\alpha} q_1^\mu\\
&+ \Big[\underbrace{\Big(\mathrm{Re}(C_S C_P^*)(4y(z+2x)m_\mu) + i\,\mathrm{Im}(C_S C_P^*)4m_F y\Big)}_{(\mathrm{I})_\beta} q_2^\mu\\
&+ \underbrace{\Big(\mathrm{Re}\,(C_S C_P^*)(-4x(z+2y)m_\mu) + i\,\mathrm{Im}\,(C_S C_P^*)4m_F x\Big)}_{(\mathrm{II})_\beta} q_1^\mu\\
&+ \mathrm{Re}\,(C_S C_P^*)(k^2 - 2xyp^2 + 2z^2m_\mu^2 - 2m_F^2)\gamma^\mu\Big]\gamma^5\\
&+ \Big(\big(-\frac{1}{2}k^2 + xyp^2 + z(2-z)m_\mu^2 + m_F^2\big)(|C_S|^2 + |C_P|^2)\\
&+ 2m_F m_\mu(|C_S|^2 - |C_P|^2)\Big)\gamma^\mu\Big]u(q_1).\end{aligned} \tag{3.1.25}$$

In order to apply the Gordan identity, the linear combinations a and b as in Eq. (2.4.30) are formed again. For the terms relevant to the magnetic or electric form factor, identified

by α, we derive

$$a_\alpha = z(x-y)m_\mu(|C_S|^2+|C_P|^2) + m_F(x-y)(|C_S|^2-|C_P|^2) \tag{3.1.26}$$

and

$$\begin{aligned} b_\alpha &= z(-x-y)m_\mu(|C_S|^2+|C_P|^2) + m_F(-x-y)(|C_S|^2-|C_P|^2) \\ &\overset{(2.4.9)}{=} z(z-1)m_\mu(|C_S|^2+|C_P|^2) + (z-1)(|C_S|^2-|C_P|^2). \end{aligned} \tag{3.1.27}$$

To ensure completeness, we calculate the linear combinations of terms containing γ^5, labeled as β, in the same way, leading to

$$\begin{aligned} a_\beta &= 2\,\mathrm{Re}\,(C_S C_P^*)[y(2x+z)+x(z+2y)]m_\mu + 2i\,\mathrm{Im}(C_S C_P^*)(y-x)m_F \\ &\overset{(2.4.9)}{=} 2\,\mathrm{Re}(C_S C_P^*)[4xy+z(1-z)]m_\mu + 2i\,\mathrm{Im}(C_S C_P^*)(y-x)m_F \end{aligned} \tag{3.1.28}$$

and

$$\begin{aligned} b_\beta &= 2\,\mathrm{Re}(C_S C_P^*)[y(z+2x)-x(z+2y)]m_\mu + 2i\,\mathrm{Im}(C_S C_P^*)(x+y)m_F \\ &\overset{(2.4.9)}{=} 2\,\mathrm{Re}(C_S C_P^*)z(y-x)m_\mu + 2i\,\mathrm{Im}(C_S C_P^*)(1-z)m_F. \end{aligned} \tag{3.1.29}$$

Applying the Gordon decomposition results in

$$\begin{aligned} N'^\mu = \bar{u}(q_2)\Big[&\Big(z(x-y)m_\mu(|C_S|^2+|C_P|^2) + (x-y)m_F(|C_S|^2-|C_P|^2)\Big)\,p^\mu \\ &+\Big(\big(-\frac{1}{2}k^2+xyp^2+z(2-z)m_\mu^2+m_F^2\big)(|C_S|^2+|C_P|^2) + 2m_F m_\mu(|C_S|^2-|C_P|^2)\Big)\gamma^\mu \\ &\quad + 2m_\mu\Big(z(z-1)m_\mu(|C_S|^2+|C_P|^2) + (z-1)m_F(|C_S|^2-|C_P|^2)\Big)\,\gamma^\mu \\ &\quad - i\Big(z(z-1)m_\mu(|C_S|^2+|C_P|^2) + (z-1)m_F(|C_S|^2-|C_P|^2)\Big)\,\sigma^{\mu\nu}p_\nu \\ &\quad - i\Big(2\,\mathrm{Re}\,(C_S C_P^*)z(y-x)m_\mu + 2i\,\mathrm{Im}\,(C_S C_P^*)(1-z)m_F\Big)\sigma^{\mu\nu}p_\nu\gamma^5 \\ &\quad + \Big(2\,\mathrm{Re}\,(C_S C_P^*)[4xy+z(1-z)]m_\mu + 2i\,\mathrm{Im}\,(C_S C_P^*)(y-x)m_F\Big)p^\mu\gamma^5 \\ &\quad + \mathrm{Re}(C_S C_P^*)\left(k^2-2xyp^2+2z^2m_\mu^2-2m_F^2\right)\gamma^\mu\gamma^5\Big]u(q_1). \end{aligned} \tag{3.1.30}$$

The antisymmetric terms under the exchange $x \leftrightarrow y$ vanish after integrating over the Feynman parameters, allowing us to directly discard these terms. Consequently, the numerator simplifies to

$$\begin{aligned} N'^\mu = \bar{u}(q_2)\Big[&\Big(\big(-\frac{1}{2}k^2+xyp^2+z^2m_\mu^2+m_F^2\big)(|C_S|^2+|C_P|^2) + 2zm_F m_\mu(|C_S|^2-|C_P|^2)\Big)\,\gamma^\mu \\ &\quad - i\Big(z(z-1)m_\mu(|C_S|^2+|C_P|^2) + (z-1)m_F(|C_S|^2-|C_P|^2)\Big)\,\sigma^{\mu\nu}p_\nu \\ &\quad + 2\,\mathrm{Im}\,(C_S C_P^*)(1-z)m_F\sigma^{\mu\nu}p_\nu\gamma^5 \\ &\quad + 2\,\mathrm{Re}(C_S C_P^*)(4xy+z(1-z))m_\mu p^\mu\gamma^5 \\ &\quad + \mathrm{Re}(C_S C_P^*)\left(k^2-2xyp^2+2z^2m_\mu^2-2m_F^2\right)\gamma^\mu\gamma^5\Big]u(q_1). \end{aligned} \tag{3.1.31}$$

By comparing this expression with Eq. (2.3.11), we can determine the magnetic form factor as

$$F(p^2) = -\frac{2m_\mu}{e}2Q_F e(-i)\int\frac{d^4k}{(2\pi)^4}\int_0^1 dx\,dy\,dz\,\delta(x+y+z-1)$$

$$\times \frac{z(z-1)m_\mu(|C_S|^2+|C_P|^2)+(z-1)m_F(|C_S|^2-|C_P|^2)}{[k^2-\Delta+i\epsilon]^3}$$

$$\overset{(2.4.38)}{=} \frac{4m_\mu Q_F}{32\pi^2}\int_0^1 dx\,dy\,dz\,\delta(x+y+z-1)$$

$$\times \frac{z(z-1)m_\mu(|C_S|^2+|C_P|^2)+(z-1)m_F(|C_S|^2-|C_P|^2)}{-xyp^2+(1-z)m_F^2+(z^2-z)m_\mu^2+zm_H^2}. \tag{3.1.32}$$

Performing the non-relativistic limit and inserting $p^2 = 0$ leads, after evaluating the δ-function, to

$$F_M(0) = \frac{Q_F}{8\pi^2}\int_0^1 dz\int_0^{1-z} dy\,\frac{z(z-1)\left(|C_S|^2+|C_P|^2\right)+(z-1)\frac{m_F}{m_\mu}\left(|C_S|^2-|C_P|^2\right)}{(1-z)m_F^2+(z^2-z)m_\mu^2+zm_H^2}$$

$$= -\frac{Q_F m_\mu^2}{8\pi^2}\int_0^1 dz\int_0^{1-z} dy\,\frac{\left(z(1-z)+\frac{m_F}{m_\mu}(1-z)\right)|C_S|^2+\left(z(1-z)-\frac{m_F}{m_\mu}(1-z)\right)|C_P|^2}{(1-z)\frac{m_F^2}{m_\mu^2}+(1-z)^2-(1-z)+z\frac{m_H^2}{m_\mu^2}}. \tag{3.1.33}$$

Carrying out the y-integration and substituting $z \to 1-z$ yields the anomalous magnetic moment:

$$[a_\mu]_a = F_M(0) = -\frac{Q_F}{8\pi^2}\int_0^1 dz\,\frac{\left(z^2(1-z)+\Lambda_F z^2\right)|C_S|^2+\left(z^2(1-z)-\Lambda_F z^2\right)|C_P|^2}{z^2+z(\Lambda_F^2-1)+\Lambda_H^2(1-z)}. \tag{3.1.34}$$

Here, we swapped the integration bounds after substitution and introduced $\Lambda_i = \frac{m_i}{m_\mu}$ for $i = F, H$. The result can be reproduced with the publicly accessible *Package*-`X` in *Mathematica*. This is demonstrated in Appendix A.12.

3.2 Photoemission from the Internal Scalar Line

In contrast to the previously examined scenario of photoemission from an internal charged fermion line, photoemission can also occur from an internal scalar line if the current model includes a charged scalar (refer to Fig. 3b).
The invariant amplitude $\mathcal{M} = \epsilon_\mu \mathcal{M}^\mu$ is given by

$$i\mathcal{M}^\mu = \int \frac{d^4k}{(2\pi)^4}\,\bar{u}(q_2)i(C_S+C_P\gamma^5)\frac{i(\not{q}_1-\not{k}+m_F)}{(q_1-k)^2-m_F^2+i\epsilon}\frac{i}{(p+k)^2-m_H^2+i\epsilon}(iQ_H e(2k+p)^\mu)$$

$$\times \frac{i}{k^2-m_H^2+i\epsilon}i(C_S^*-C_P^*\gamma^5)u(q_1). \tag{3.2.1}$$

The associated contribution to the muon's AMM can be determined with *Package*-`X`, discussed in Appendix A.12. The calculation yields

$$[a_\mu]_b = -\frac{Q_H}{8\pi^2}\int_0^1 dz\,\frac{\left(z^2(z-1)+\Lambda_F(z^2-z)\right)|C_S|^2+\left(z^2(z-1)-\Lambda_F(z^2-z)\right)|C_P|^2}{z^2+\Lambda_F^2(1-z)+z(\Lambda_H^2-1)}. \tag{3.2.2}$$

In the SM, it should be highlighted that the sole contribution arises from the photoemission occurring along the internal charged fermion line, since there are no charged scalars present in the SM. In the following sections, we will add some scalars to the SM to explain the $\Delta a_\mu = (2.49 \pm 0.48) \times 10^{-9}$ discrepancy between theory and experiment.

4 The Two-Higgs-Doublet Model

One of the simplest extensions of the SM is the 2HDM. In the SM, there is a simple scalar structure consisting of one SU(2) doublet. This model extends that structure to two doublets.
The 2HDM has been extensively studied in the literature due to its many possible applications [15]. One of the main reasons for considering the 2HDM is its significance in supersymmetric theories [16]. In these models, a single Higgs doublet can generate the mass of quarks only with one type of charge. Therefore, supersymmetric frameworks like the Minimal Supersymmetric Standard Model require at least two Higgs doublets [7]. Another motivation for the 2HDM is that the SM cannot describe the baryon asymmetry of the universe. This asymmetry, which explains the observed dominance of matter over antimatter in the universe, is due to CP-violation, which is insufficiently pronounced in the SM [1].

4.1 Introduction to the Model

We add a second SU(2) doublet Φ_2 to the existing SM doublet Φ_1. Each doublet carries hypercharge $Y = 1/2$.[2] Both exhibit vacuum expectation values (VEVs):

$$\langle \Phi_1 \rangle_0 = \begin{pmatrix} 0 \\ \frac{v_1}{\sqrt{2}} \end{pmatrix}, \qquad \langle \Phi_2 \rangle_0 = \begin{pmatrix} 0 \\ \frac{v_2}{\sqrt{2}} \end{pmatrix} \tag{4.1.1}$$

We perform a rotation by the angle β to achieve a particularly convenient rotated basis. After rotation, the doublets denoted H_1 and H_2 are obtained, with only one neutral Higgs (H_1^0) having a nonzero VEV. To achieve this so-called Higgs basis, we rotate the original basis by $\beta = \arctan v_2/v_1$:

$$\begin{pmatrix} H_1 \\ H_2 \end{pmatrix} = \begin{pmatrix} \cos\beta & \sin\beta \\ -\sin\beta & \cos\beta \end{pmatrix} \begin{pmatrix} \Phi_1 \\ \Phi_2 \end{pmatrix}. \tag{4.1.2}$$

The nonzero VEV is now represented by $v = \sqrt{v_1^2 + v_2^2} \simeq 246\,\mathrm{GeV}$. The most general scalar potential in this rotated Higgs basis is given by [17, p. 45]

$$\begin{aligned} V = {} & m_{11}^2 H_1^\dagger H_1 + m_{22}^2 H_2^\dagger H_2 - \left(m_{12}^2 H_1^\dagger H_2 + \mathrm{H.c.} \right) \\ & + \frac{\lambda_1}{2} \left(H_1^\dagger H_1 \right)^2 + \frac{\lambda_2}{2} \left(H_2^\dagger H_2 \right)^2 + \lambda_3 \left(H_1^\dagger H_1 \right) \left(H_2^\dagger H_2 \right) + \lambda_4 \left(H_1^\dagger H_2 \right) \left(H_2^\dagger H_1 \right) \\ & + \left[\frac{\lambda_5}{2} \left(H_1^\dagger H_2 \right)^2 + \left[\lambda_6 \left(H_1^\dagger H_1 \right) + \lambda_7 \left(H_2^\dagger H_2 \right) \right] H_1^\dagger H_2 + \mathrm{H.c.} \right]. \end{aligned} \tag{4.1.3}$$

Here, m_{12}^2 and $\lambda_{5,6,7}$ can generally be complex, while the remaining parameters are real. We work in the CP-conserving limit, assuming all parameters to be real [18, p. 210].
As a result of the two SU(2) doublets, there are 8 fields:

$$H_1 = \begin{pmatrix} G^+ \\ \frac{1}{\sqrt{2}}(v + H_1^0 + iG^0) \end{pmatrix}, \qquad H_2 = \begin{pmatrix} H^+ \\ \frac{1}{\sqrt{2}}(H_2^0 + iA^0) \end{pmatrix}. \tag{4.1.4}$$

The G^+ and G^0 are Goldstone bosons that get 'eaten' by the $W^\pm$ and Z^0 gauge bosons, thus acquiring a third polarization and gaining mass. Consequently, five physical scalars

[2] In some literature, the convention $Y = 1$ is used. Since hypercharge is not a directly measurable quantity, consistency within the chosen convention is essential.

remain.
As can be seen from the neutral scalar mass matrix (see Appendix A.13), because the parameters λ_4 and λ_5 are real in the CP-conserving limit, the CP-odd eigenstate decouples from the CP-even eigenstates. However, the two CP-even eigenstates mix to form

$$\begin{pmatrix} h \\ H \end{pmatrix} = \begin{pmatrix} \cos(\alpha-\beta) & \sin(\alpha-\beta) \\ -\sin(\alpha-\beta) & \cos(\alpha-\beta) \end{pmatrix} \begin{pmatrix} H_1^0 \\ H_2^0 \end{pmatrix}, \tag{4.1.5}$$

where the angle $(\alpha-\beta)$, which diagonalizes the CP-even mass matrix, is given by:

$$\sin 2(\alpha-\beta) = \frac{2\lambda_6 v^2}{m_H^2 - m_h^2}. \tag{4.1.6}$$

The conventional choice of the angle $\alpha-\beta$ results from the fact that a rotation by the angle β has already been made during the transformation into the Higgs basis. In the chosen alignment limit, the corresponding choice is $\alpha \approx \beta$. Under this consideration, the SM Higgs ($h \approx H_1^0$) approximately decouples from the 'new' CP-even state ($H \approx H_2^0$).
In the considered limit of the model, we obtain (see Appendix A.13):

$$m_h^2 = \lambda_1 v^2, \qquad m_H^2 = m_{22}^2 + \frac{v^2}{2}\left(\lambda_3+\lambda_4+\lambda_5\right), \tag{4.1.7}$$

$$m_A^2 = m_H^2 - v^2\lambda_5, \qquad m_{H^\pm}^2 = m_H^2 - \frac{v^2}{2}\left(\lambda_4+\lambda_5\right). \tag{4.1.8}$$

It is important to mention that the electroweak data have constrained the parameter space. Due to the absence of non-SM events, the mass of the charged scalar H^+ has a lower bound [19]. Therefore, $m_{H^+} \geq 110\,\text{GeV}$ is chosen. The masses of the neutral scalars are also constrained. The experimentally investigated $Z \to HA$ decay imposes the condition $m_A + m_H > m_Z \approx 91\,\text{GeV}$, which means that both neutral scalars cannot be simultaneously light. When analyzing the respective contributions to the AMM, it will turn out that $\Delta m = m_{H^+,A} - m_H = 110\,\text{GeV}$ provides a possible suitable choice. We adopt the degenerate scenario $m_{H^+} = m_A$, which ensures that the masses chosen in subsequent analyzes comply with the constraints of the T parameter [20].
For the parameters in Eqs. (4.1.7) and Eqs. (4.1.8), $\lambda_4 = \lambda_5 \equiv \lambda$ therefore applies. This results in $m_A^2 = m_{H^+}^2 = m_H^2 - v^2\lambda$. For triple scalar couplings, λ occurs as a coupling parameter [21]. In order to validate the applicability of perturbation theory, $|\lambda| < 4\pi$ imposes a limit on the maximal mass difference Δm, dependent on m_H.[3] The most stringent condition exists for the highest investigated scalar mass $m_H = 1000\,\text{GeV}$ and results in $\Delta m \lesssim 325\,\text{GeV}$. Selecting $\Delta m = 110\,\text{GeV}$ leads to a parameter of $\lambda = -0.200$ ($\lambda = -3.835$) for $m_H = 0$ ($m_H = 1000\,\text{GeV}$).

The Yukawa interactions of the leptons with the physical scalars are given by [22]:

$$-\mathcal{L}_{\text{Yuk}} \supset \widetilde{Y}_{ij}\overline{L}_{L_i} H_1 \ell_{R_j} + Y_{ij}\overline{L}_{L_i} H_2 \ell_{R_j} + \text{H.c.} \tag{4.1.9}$$

with the left-handed doublet $L_L = (\nu, \ell)_L^T$ and right-handed singlet ℓ_R . The indices i and j represent the three lepton generations. As only H_1 has a nonzero VEV in the Higgs basis, the masses of the charged leptons are given by $M_{ij} = \frac{v}{\sqrt{2}}\widetilde{Y}_{ij}$. Since Y and $\widetilde{Y}$ are independent 3×3 coupling matrices, we can choose the mass matrix M, and thus $\widetilde{Y}$, to

[3] The constraint $|\lambda| < 4\pi$ is rather lenient and is often made more stringent. Smaller values of the parameter lead to faster convergence of the perturbation series.

be real and diagonal.
In the following analysis, we examine different cases of the Yukawa coupling matrix Y, where the matrix elements are chosen to be real. Because Y_{ij} is independent of $\widetilde{Y}_{ij}$ (and thus independent of M_{ij}), the couplings Y_{ij} are not correlated with the lepton masses.
Since all new physical scalars are in the same doublet H_2, the lepton Yukawa couplings for the physical scalars are determined by:

$$-\mathcal{L}_{\text{Yuk}} \supset \frac{1}{\sqrt{2}}\left[Y_{ij}H^0 + iY_{ij}A^0\right]\bar{\ell}_{L_i}\ell_{R_j} + Y_{ij}\bar{\nu}_{L_i}\ell_{R_j}H^+ + \text{H.c.} \tag{4.1.10}$$

4.2 Anomalous Magnetic Moment for Different Textures of the Yukawa Coupling Matrix

The model under discussion includes one charged scalar (H^+) along with three neutral scalars (h, H, A). In the alignment limit adopted, h is identified with the SM Higgs, and thus its contribution is already included in a_μ^{SM}. We explore various coupling scenarios defined by the Yukawa coupling matrix Y. The general Yukawa coupling matrix can be written as

$$Y = \begin{pmatrix} Y_{ee} & Y_{e\mu} & Y_{e\tau} \\ Y_{\mu e} & Y_{\mu\mu} & Y_{\mu\tau} \\ Y_{\tau e} & Y_{\tau\mu} & Y_{\tau\tau} \end{pmatrix}. \tag{4.2.1}$$

The different textures considered are given by the following matrices:

$$\text{tex. 1:}\quad Y = \begin{pmatrix} 0 & 0 & 0 \\ 0 & Y_{\mu\mu} & 0 \\ 0 & 0 & 0 \end{pmatrix}, \qquad \text{tex. 2:}\quad Y = \begin{pmatrix} 0 & 0 & 0 \\ 0 & 0 & 0 \\ 0 & Y_{\tau\mu} & 0 \end{pmatrix},$$

$$\text{tex. 3:}\quad Y = \begin{pmatrix} 0 & Y_{e\mu} & 0 \\ 0 & 0 & 0 \\ 0 & 0 & 0 \end{pmatrix}, \qquad \text{tex. 4:}\quad Y = \begin{pmatrix} 0 & 0 & 0 \\ 0 & 0 & Y_{\mu\tau} \\ 0 & Y_{\tau\mu} & 0 \end{pmatrix}.$$

For each case, we use the derived one-loop corrections through Eq. (3.1.34) and Eq. (3.2.2). To express the scalar (pseudoscalar) coupling constants C_S (C_P) by the Yukawa couplings Y_{ij}, the Lagrangian in Eq. (3.0.1) and Eq. (4.1.10) are compared.

4.2.1 Texture 1: Diagonal Yukawa Coupling Matrix

In the first scenario, we assume the Yukawa coupling matrix to be diagonal. For this choice, the Yukawa interactions with the new physical scalars are given by:

$$-\mathcal{L}_{\text{Yuk}} \supset \frac{1}{\sqrt{2}}\left[Y_{\mu\mu}H^0 + iY_{\mu\mu}A^0\right]\bar{\mu}_L\mu_R + Y_{\mu\mu}\bar{\nu}_{L\mu}\mu_R H^+ + \text{H.c.} \tag{4.2.2}$$

To compute the Hermitian conjugate, we expand the Lagrangian via left- and right-handed projectors (see Appendix A.11):

$$\begin{aligned} \text{H.c.} &= \left[\frac{1}{\sqrt{2}}[Y_{\mu\mu}H^0 + iY_{\mu\mu}A^0]\bar{\mu}_L\mu_R + Y_{\mu\mu}\bar{\nu}_{L\mu}\mu_R H^+\right]^\dagger \\ &= \frac{1}{\sqrt{2}}Y_{\mu\mu}[H^0 - iA^0]\mu^\dagger\left(\frac{1+\gamma^5}{2}\right)\gamma^0\mu + Y_{\mu\mu}H^-\mu^\dagger\left(\frac{1+\gamma^5}{2}\right)\gamma^0\nu_\mu \\ &= \frac{1}{2\sqrt{2}}Y_{\mu\mu}[H^0 - iA^0]\bar{\mu}(1-\gamma^5)\mu + \frac{1}{2}Y_{\mu\mu}H^-\bar{\mu}(1-\gamma^5)\nu_\mu. \end{aligned} \tag{4.2.3}$$

For the neutral scalars, we combine this expression with the stated terms in Eq. (4.2.2). The Hermitian conjugate of the charged scalar part does not contribute additionally, as it corresponds to the same Feynman diagram with reversed momentum direction for the H^+ scalar. A comparison with the Lagrangian (3.0.1) indicates that they represent distinct directions for the charged scalar's momentum. Therefore, to include the contribution from the charged scalar, as outlined in Eq. (3.2.2), it is necessary to use $Q_{H^+} = -1$. To maintain alignment with the standard convention of H^+, the contribution will retain its current label. Altogether, the relevant part of the Lagrangian is given by

$$\begin{aligned} -\mathcal{L}_{\text{Yuk}} \supset & \frac{Y_{\mu\mu}}{2\sqrt{2}}[H^0 + iA^0]\bar{\mu}(1+\gamma^5)\mu + \frac{Y_{\mu\mu}}{2\sqrt{2}}[H^0 - iA^0]\bar{\mu}(1-\gamma^5)\mu + \frac{Y_{\mu\mu}}{2}\bar{\mu}_R\nu_{L\mu}H^- \\ = & \frac{1}{\sqrt{2}}Y_{\mu\mu}\bar{\mu}\mu H^0 + \frac{i}{\sqrt{2}}Y_{\mu\mu}\bar{\mu}\gamma^5\mu A^0 + \frac{1}{2}Y_{\mu\mu}\bar{\mu}(1-\gamma^5)\nu_\mu H^-. \end{aligned} \tag{4.2.4}$$

A comparison with the Lagrangian in Eq. (3.0.1) leads to the scalar and pseudoscalar coefficients:

$$C_S(H^0) = \frac{1}{\sqrt{2}}Y_{\mu\mu}, \qquad C_P(H^0) = 0, \tag{4.2.5}$$

$$C_S(A^0) = 0, \qquad C_P(A^0) = \frac{i}{\sqrt{2}}Y_{\mu\mu}, \tag{4.2.6}$$

$$C_S(H^+) = \frac{1}{2}Y_{\mu\mu}, \qquad C_P(H^+) = -\frac{1}{2}Y_{\mu\mu}. \tag{4.2.7}$$

From the Formulae (3.1.34) and (3.2.2), these relations result in the one-loop contributions of CP-even, CP-odd and the charged scalar. Note that because of the conservation of charge per vertex, $Q_\nu + Q_{H^+} = Q_\mu$ must hold. This condition is satisfied with $Q_\mu = Q_{H^+} = -1$, yielding the subsequent outcomes for the new scalar contributions:

$$\Delta a_\mu^H = \frac{Y_{\mu\mu}^2}{16\pi^2}\int_0^1 dz\, \frac{z^2(2-z)}{z^2 + \Lambda_H^2(1-z)} \tag{4.2.8}$$

$$\simeq \frac{Y_{\mu\mu}^2}{16\pi^2}\begin{cases} \frac{1}{\Lambda_H^2}\ln\Lambda_H^2 & \text{for} \quad \Lambda_H \gg 1 \\ \frac{3}{2} & \text{for} \quad \Lambda_H \ll 1 \end{cases}, \tag{4.2.9}$$

$$\Delta a_\mu^A = \frac{Y_{\mu\mu}^2}{16\pi^2}\int_0^1 dz\, \frac{-z^3}{z^2 + \Lambda_A^2(1-z)} \tag{4.2.10}$$

$$\simeq -\frac{Y_{\mu\mu}^2}{16\pi^2}\begin{cases} \frac{1}{\Lambda_A^2}\ln\Lambda_A^2 & \text{for} \quad \Lambda_A \gg 1 \\ \frac{1}{2} & \text{for} \quad \Lambda_A \ll 1 \end{cases}, \tag{4.2.11}$$

$$\Delta a_\mu^{H^+} = \frac{Y_{\mu\mu}^2}{16\pi^2}\int_0^1 dz\, \frac{z^2(z-1)}{z^2 + z(\Lambda_{H^+}^2 - 1)} \tag{4.2.12}$$

$$\simeq -\frac{Y_{\mu\mu}^2}{16\pi^2}\begin{cases} \frac{1}{6\Lambda_{H^+}^2} & \text{for} \quad \Lambda_{H^+} \gg 1 \\ \left(-\frac{1}{2}\right) & \text{for} \quad \Lambda_{H^+} \ll 1 \end{cases}. \tag{4.2.13}$$

Here, $\Lambda_S = m_S/m_\mu$ for $S = H, A, H^+$ is implemented. The corresponding Lagrangian term indicates that the fermion in the charged scalar contribution is a neutrino, thus the corresponding mass term has been neglected in the derivation. To simplify the analysis of the various contributions, we employed approximations for both large and small scalar masses. A derivation of the non-trivial approximation for neutral scalars at large scalar masses is provided in the Appendix A.14.

The various contributions are illustrated in Figure 4a. For the integrations, the *scipy.integrate* Python library [23] was used. The CP-even scalar H adds positively to Δa_μ, in contrast to the CP-odd scalar A, which adds negatively. In both scenarios, the denominator of the integrand is positive. For Δa_μ^H, the positive contribution arises from the dominant term $2z^2$ in the numerator. As illustrated in Eq. (4.2.9) and Eq. (4.2.11), for lower scalar masses, the contribution Δa_μ^H is more prominent than Δa_μ^A. However, at higher scalar masses, both contributions equalize in magnitude. On the other hand, for the charged scalar contribution, a negative contribution results for $m_{H^+} > m_\mu$ ($\Lambda_{H^+} > 1$). For $\Lambda_{H^+} < 1$ oscillatory behavior is present. This is clear from the presence of poles within the interval $0 \leq z \leq 1$, which are necessary to achieve the sign flip noted in the related approximations.
To explain the positive discrepancy in Δa_μ, we choose a mass hierarchy where $m_H \ll m_A, m_{H^+}$. With this choice, the negative contributions of Δa_μ^A and $\Delta a_\mu^{H^+}$ are reduced. In particular, we select the mass difference $\Delta m = m_{A,H^+} - m_H = 110\,\text{GeV}$ as discussed in Sec. 4.1, ensuring it aligns with the experimental constraints.
In Figure 4b two different mass splittings $\Delta m = m_{A,H^+} - m_H$ are shown. It is evident that as the mass split increases, the absolute values of the negative contributions Δa_μ^A and $\Delta a_\mu^{H^+}$ decrease. Up to the order of magnitude of the mass split $\mathcal{O}(\Delta m)$, the total Δa_μ is predominantly influenced by Δa_μ^H.

Figure 5 illustrates which masses m_H and Yukawa couplings $Y_{\mu\mu}$ fulfill the 1σ or 2σ range of Δa_μ. For this purpose, 50 000 random parameter combinations were analyzed in the shown parameter space. As higher-order contributions form a perturbation series in $\frac{Y_{\mu\mu}^2}{16\pi^2}$, an upper limit on the Yukawa couplings is required for convergence. Hence, we set $Y_{\mu\mu} \leq 1$ for the parameter scan. The shape of the curve is expected due to the reduced contributions with increasing scalar masses. Consequently, larger couplings are needed to compensate for this decrease.
Experimental data exclude specific regions of the parameter space, as shown in Fig. 5 with shaded regions. Notably, E137 imposes significant constraints on $m_H < 2m_\mu$ [24]. Although higher masses currently have fewer regions excluded, many of these areas will probably be disqualified by upcoming experiments or analyzes.

4.2.2 Texture 2 & 3: One Off-Diagonal Yukawa Coupling Matrix Element

In contrast to utilizing a diagonal Yukawa coupling matrix as discussed in the previous section, we can also examine the effects of non-diagonal Yukawa coupling matrices on the AMM contributed by the new scalars. The subsequent analysis investigates both the texture 2 and texture 3 structures. As the two scenarios only differ in the respective fermion masses, $\ell = \tau, e$ is used subsequently. The corresponding Yukawa Lagrangian is given by:

$$-\mathcal{L}_{\text{Yuk}} \supset \frac{1}{\sqrt{2}}[Y_{\ell\mu}H^0 + iY_{\ell\mu}A^0]\bar{\ell}_L\mu_R + Y_{\ell\mu}\bar{\nu}_{L\ell}\mu_R H^+ + \text{H.c.} \tag{4.2.14}$$

Notice that if only $Y_{\mu\ell}$ were present as a non-vanishing matrix element, there would be no charged scalar contribution. The corresponding Lagrangian term then contains no muon interaction. To determine the scalar (pseudoscalar) coefficients C_S (C_P), it is necessary to form the hermitian conjugate:

$$\text{H.c.} = \frac{1}{2\sqrt{2}}Y_{\ell\mu}[H^0 - iA^0]\bar{\mu}\Big(1-\gamma^5\Big)\ell + \frac{1}{2}Y_{\ell\mu}\bar{\mu}\Big(1-\gamma^5\Big)\nu_\ell H^-. \tag{4.2.15}$$

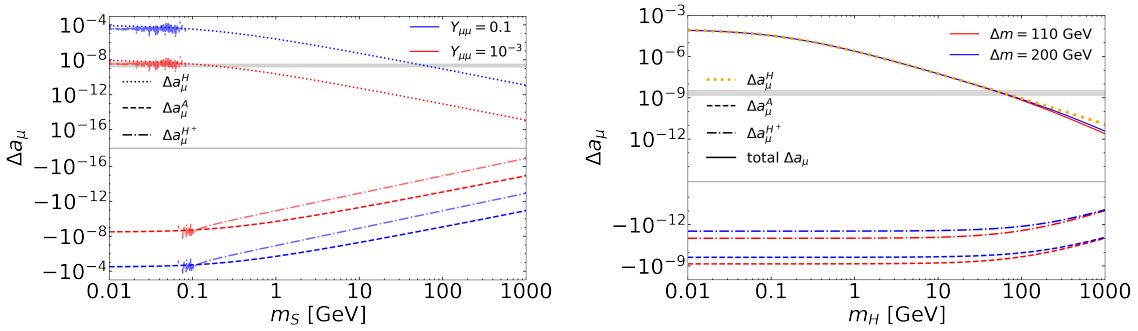

(a) (b)

Figure 4: Contribution of the CP-even scalar (dotted), the CP-odd scalar (dashed), and the charged scalar (dash-dotted) to Δa_μ for texture 1. The gray-shaded area represents the experimental allowed 2σ region of Δa_μ. Individual contributions for $Y_{\mu\mu} = 0.1$ (blue) and $Y_{\mu\mu} = 10^{-3}$ (red) depending on m_S with $S = H, A, H^+$ are shown on the left. The right plot illustrates the individual and total contribution Δa_μ (solid line) concerning a specific mass hierarchy of $\Delta m = m_{A,H^+} - m_H = 110\,\text{GeV}$ (red) and $\Delta m = m_{A,H^+} - m_H = 200\,\text{GeV}$ (blue) for $Y_{\mu\mu} = 0.1$.

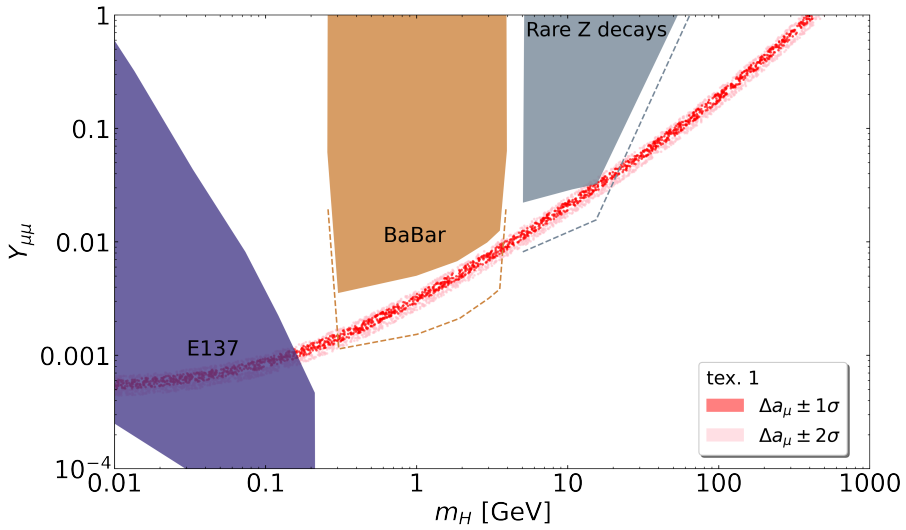

Figure 5: Possible parameter combinations to match the 1σ (red) or 2σ (pink) range of Δa_μ. The mass hierarchy is chosen as $\Delta m = m_{A,H^+} - m_H = 110\,\text{GeV}$. Various restrictions are shown by colored areas that exclude the relevant parameter space. The constraints shown are from CMS (gray shaded) [25], BaBar (brown shaded) [26] and SLAC beam dump E137 (blue shaded) [24]. In addition, there are projected sensitivity ranges that will be investigated in future experiments and/or analyzes. Shown are HL-LHC (gray dashed line) and Belle-II (brown dashed line) [27]. The constraints are taken from [28].

Now, the Lagrangian structure matches that provided in Eq. (3.0.1), implying that:

$$C_S(H) = -C_P(H) = \frac{Y_{\ell\mu}}{2\sqrt{2}}, \tag{4.2.16}$$

$$C_S(A) = -C_P(A) = -i\frac{Y_{\ell\mu}}{2\sqrt{2}}, \tag{4.2.17}$$

$$C_S(H^+) = -C_P(H^+) = \frac{1}{2}Y_{\ell\mu}. \tag{4.2.18}$$

Plugging these results into Eq. (3.1.34) and Eq. (3.2.2) yields

$$\Delta a_\mu^\phi = \frac{Y_{\ell\mu}^2}{32\pi^2}\int_0^1 dz \frac{z^2(1-z)}{z^2 + z(\Lambda_\ell^2 - 1) + \Lambda_\phi^2(1-z)} \tag{4.2.19}$$

$$\simeq \frac{Y_{\ell\mu}^2}{32\pi^2}\begin{cases} \frac{1}{3\Lambda_\phi^2} & \text{for} \quad \Lambda_\phi \gg 1, \Lambda_\ell \\ \frac{1}{6\Lambda_\ell^2} & \text{for} \quad \Lambda_\ell \gg 1, \Lambda_\phi \\ \left(-\frac{1}{2}\right) & \text{for} \quad \Lambda_\ell, \Lambda_H \ll 1 \end{cases}. \tag{4.2.20}$$

Here, $\phi = H, A$ is introduced. The contribution from the charged scalar aligns with that of texture 1 and can thus be expressed by Eq. (4.2.12) with the respective Yukawa coupling $Y_{\ell\mu}$. In the case of the neutral scalar, an additional distinction was made to highlight the differences between texture 2 ($\Lambda_\tau \gg 1$) and texture 3 ($\Lambda_e \ll 1$). For both textures, with the approximations in Eq. (4.2.13) and Eq. (4.2.20), it is evident that the magnitudes of the neutral and charged scalar contributions differ only for small scalar masses m_S. The rate at which the contributions converge is determined by the lepton mass m_ℓ. Furthermore, the approximations indicate that for the electron-muon coupling (texture 3) the neutral scalar yields a negative contribution when the scalar mass is small. The change in sign occurs in the denominator, causing oscillations similar to those seen in the charged scalar contribution. The respective contributions for $\ell = \tau, e$ are shown in Fig. 6.

To explain the experimental value of the AMM using one of these textures, it is necessary to choose a mass hierarchy of the form $m_H \ll m_{H^+}$. Based on the aforementioned constraints, $m_H + m_A > m_Z$ is required. Since the two neutral-scalar contributions are equal, the light scalar can be chosen freely. The mass hierarchy of the form $\Delta m = m_{A,H^+} - m_H = 110\,\text{GeV}$ is chosen again. The corresponding parameter scan can be seen in Fig. 7. There are notable distinctions between texture 2 and texture 3 when the scalar masses are below $m_H \lesssim 10\,\text{GeV}$. In particular, the electron case shows that there are no possible parameter combinations at $m_H \lesssim m_\mu$. This phenomenon arises because the contribution in this limit becomes negative.

In addition to the theoretically allowed parameter combinations, the experimental constraints are illustrated by the excluded regions in Fig. 7. For texture 2, the parameter range for $m_H < m_\tau - m_\mu$ is forbidden due to the $\tau \to \mu H$ decay investigated at ARGUS [29]. In contrast, the Yukawa coupling in texture 3 faces restrictions based on the $e^+e^- \to \mu^+\mu^-$ data from LEP [30] and the data from CMS [31]. Furthermore, to avoid $Z \to 4\ell$ decay, certain regions in the parameter space are excluded [32].

In contrast to the scenario with a diagonal Yukawa coupling matrix (texture 1), it is evident that the use of an off-diagonal Yukawa coupling matrix element, as seen in textures 2 and texture 3, leads to reduced contributions and thus requires stronger couplings

to match the experimental value of the AMM (see Fig. 10). A comparison of the approximations for the dominant CP-even contributions in Eq. (4.2.9) and Eq. (4.2.20) reveals the differences. In scenarios with large masses, the diagonal case (texture 1) includes a significant additional $6 \ln \Lambda_H^2$ factor. At lower mass regimes, the off-diagonal configuration is subject to either a suppression effect by a factor of $1/(18\Lambda_\tau^2)$ (texture 2) or yields a negative contribution (texture 3).

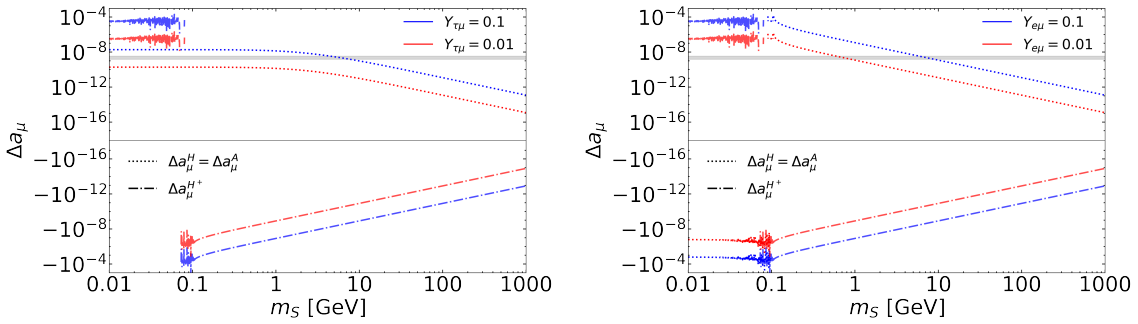

(a) (b)

Figure 6: Contribution of the CP-even scalar (dotted), the CP-odd scalar (dashed), and the charged scalar (dash-dotted) to Δa_μ. The gray-shaded area represents the experimental 2σ allowed region. Individual contributions for $Y_{\ell\mu} = 0.1$ (blue) and $Y_{\ell\mu} = 0.01$ (red) depending on m_S with $S = H, A, H^+$ are shown. The left plot illustrates texture 2 ($\ell = \tau$), while the right plot presents texture 3 ($\ell = e$).

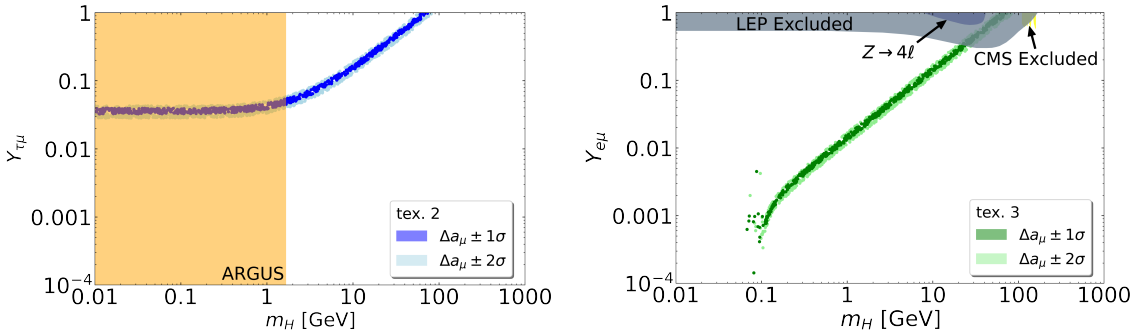

(a) (b)

Figure 7: Possible parameter configurations to match the 1σ or 2σ values of Δa_μ. The mass hierarchy is chosen as $\Delta m = m_{A,H^+} - m_H = 110\,\text{GeV}$. Shaded regions represent the parameter space excluded from experiments. The parameter space of texture 2 is excluded for $m_H < m_\tau - m_\mu$, given that investigations at ARGUS do not permit the $\tau \to \mu H$ decay [29] (left). The parameter space of texture 3 and its excluded regions are depicted in the right figure. Constraints are illustrated from LEP (gray shaded) [30], CMS (yellow shaded) [31], and the $Z \to 4\ell$ decay (blue shaded) [32]. The constraints are taken from [33, 34].

4.2.3 Texture 4: Two Off-Diagonal Yukawa Coupling Matrix Elements

The subsequent analysis will consider the scenario where the tau-muon interaction is modeled by two nonzero Yukawa matrix elements. In this case, summing over all indices in

the Lagrangian (4.1.10) leads to

$$-\mathcal{L}_{\text{Yuk}} \supset \frac{1}{\sqrt{2}}[Y_{\mu\tau}H^0 + iY_{\mu\tau}A^0]\bar{\mu}_L\tau_R + \frac{1}{\sqrt{2}}[Y_{\tau\mu}H^0 + iY_{\tau\mu}A^0]\bar{\tau}_L\mu_R + Y_{\tau\mu}\bar{\nu}_{L\tau}\mu_R H^+ + \text{H.c.} \tag{4.2.21}$$

Once again, the idea is to bring the Lagrangian into a form comparable to that of Eq. (3.0.1). Therefore, we form the Hermitian conjugate:

$$\left[\frac{1}{\sqrt{2}}[Y_{\tau\mu}H^0 + iY_{\tau\mu}A^0]\bar{\tau}_L\mu_R\right]^\dagger = \frac{1}{\sqrt{2}}[Y_{\tau\mu}H^0 - iY_{\tau\mu}A^0]\bar{\mu}_R\tau_L. \tag{4.2.22}$$

The relevant terms in the Yukawa Lagrangian are

$$\begin{aligned}-\mathcal{L}_{\text{Yuk}} &\supset \frac{1}{\sqrt{2}}[Y_{\mu\tau}H^0 + iY_{\mu\tau}A^0]\bar{\mu}_L\tau_R + \frac{1}{\sqrt{2}}[Y_{\tau\mu}H^0 - iY_{\tau\mu}A^0]\bar{\mu}_R\tau_L + Y_{\tau\mu}\bar{\mu}_R\nu_{L\tau}H^- \\ &= \frac{1}{\sqrt{2}}\bar{\mu}[Y_{\mu\tau}\mathrm{P}_R + Y_{\tau\mu}\mathrm{P}_L]H^0\tau + \frac{i}{\sqrt{2}}\bar{\mu}[Y_{\mu\tau}\mathrm{P}_R - Y_{\tau\mu}\mathrm{P}_L]A^0\tau + Y_{\tau\mu}\bar{\mu}_R\nu_{L\tau}H^-. \end{aligned} \tag{4.2.23}$$

This consequently results in the scalar and pseudoscalar coefficients:

$$C_S(H) = \frac{Y_{\mu\tau} + Y_{\tau\mu}}{2\sqrt{2}}, \qquad C_P(H) = \frac{Y_{\mu\tau} - Y_{\tau\mu}}{2\sqrt{2}}, \tag{4.2.24}$$

$$C_S(A) = i\frac{Y_{\mu\tau} - Y_{\tau\mu}}{2\sqrt{2}}, \qquad C_P(A) = i\frac{Y_{\mu\tau} + Y_{\tau\mu}}{2\sqrt{2}}, \tag{4.2.25}$$

$$C_S(H^+) = \frac{1}{2}Y_{\tau\mu}, \qquad C_P(H^+) = -\frac{1}{2}Y_{\tau\mu}. \tag{4.2.26}$$

With Formulae (3.1.34) and (3.2.2) the corresponding contributions can be derived. Due to the large tau mass ($m_\tau \gg m_\mu$), we approximate the numerator of the neutral contributions with[4]

$$x^2 - x^3 \pm \frac{m_\tau}{m_\mu} \approx \pm\frac{m_\tau}{m_\mu}. \tag{4.2.27}$$

As a result, only the mixed terms of the Yukawa coupling matrix elements (proportional to $Y_{\mu\tau}Y_{\tau\mu}$) appear in the neutral scalar contributions. The contribution from the charged scalar remains consistent across different scenarios, whereby only the matrix element $Y_{\tau\mu}$ appears in the formula. The contributions of the neutral scalars are given by

$$\Delta a_\mu^\phi = \pm\frac{Y_{\mu\tau}Y_{\tau\mu}}{16\pi^2}\Lambda_\tau \int_0^1 dz \frac{z^2}{z^2 + z(\Lambda_\tau^2 - 1) + \Lambda_\phi^2(1-z)} \tag{4.2.28}$$

$$\simeq \pm\frac{Y_{\mu\tau}Y_{\tau\mu}}{16\pi^2}\Lambda_\tau \begin{cases} \frac{1}{\Lambda_\phi^2}\ln\Lambda_\phi^2 & \text{for} \quad \Lambda_\phi \gg 1, \Lambda_\tau \\ \frac{1}{2}\frac{1}{\Lambda_\tau^2} & \text{for} \quad \Lambda_\tau \gg 1, \Lambda_\phi \end{cases}. \tag{4.2.29}$$

Here, + and − correspond to the cases $\phi = H$ and $\phi = A$, respectively. In this scenario, the Yukawa couplings can be used to freely select whether H or A contributes positively to the magnetic moment. For $Y_{\mu\tau}Y_{\tau\mu} > 0$, the CP-even contribution is positive and has the same magnitude as the negative CP-odd contribution. This choice is made without loss of generality.

[4]This approximation can only be made if there are no large ratios between $Y_{\mu\tau}$ and $Y_{\tau\mu}$. The approximation removes terms that are proportional to $Y_{\mu\tau}^2 + Y_{\tau\mu}^2$. However, we have already analyzed this scenario in the last section, with only one off-diagonal Yukawa coupling element (texture 2).

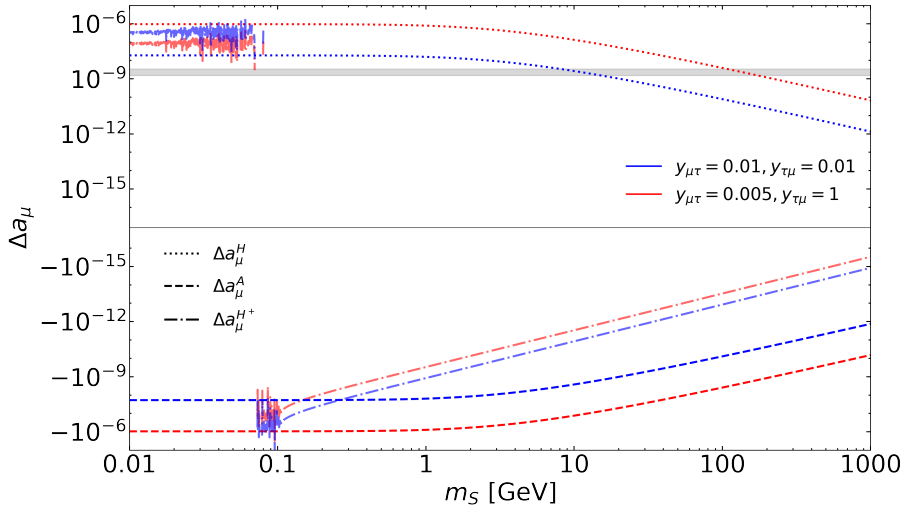

Figure 8: Contribution of the CP-even scalar (dotted), the CP-odd scalar (dashed), and the charged scalar (dash-dotted) to Δa_μ for texture 4. The gray-shaded area represents the experimental 2σ allowed region. While the neutral contributions follow the proportionality $\Delta a_\mu^{H/A} \propto Y_{\mu\tau} Y_{\tau\mu}$, the charged scalar contribution is determined by $\Delta a_\mu^{H^+} \propto Y_{\tau\mu}^2$. Consequently, the magnitudes of these contributions can be adjusted independently of each other. This is demonstrated with the coupling constants $Y_{\tau\mu} = Y_{\mu\tau} = 0.01$ (blue) and $Y_{\mu\tau} = 0.005$, $Y_{\tau\mu} = 1$ (red).

The individual contributions are illustrated in Figure 8. In this instance, a mass hierarchy is essential since the neutral contributions cancel each other out, leaving only the negative charged scalar contribution.
As a result, a mass hierarchy of the form $m_H \ll m_A$ is selected. Although $\Delta a_\mu^H = -\Delta a_\mu^A \propto Y_{\mu\tau} Y_{\tau\mu}$ but $\Delta a_\mu^{H^+} \propto Y_{\tau\mu}^2$, there are two ways to reduce the magnitude of the charged scalar contribution. The first is to increase the mass compared to the CP-even scalar, and the second is to choose a low value of the $Y_{\tau\mu}$ coupling. The issue with the second approach is that keeping $\sqrt{Y_{\mu\tau} Y_{\tau\mu}}$ constant necessitates an increase in $Y_{\mu\tau}$. Note that for couplings higher than $\mathcal{O}(1)$ the higher-order contributions are not suppressed, as more scalar fermion vertices lead to higher powers of the coupling constant. Simply looking at the first order would therefore be insufficient. Thus, we concentrate on the initial option and select $\Delta m = m_{A,H^+} - m_H = 110\,\text{GeV}$, consistent with the other textures discussed above. The corresponding parameter scan is illustrated in Figure 9. Analogue to texture 2, there is an excluded region due to the forbidden $\tau \to \mu H$ decay, which was examined at ARGUS [29].

Texture 4 of the Yukawa coupling matrix can now be compared with the other textures (see Fig. 10). The relevant curve for the allowed parameters is found to be above the diagonal coupling scenario (texture 1) for small scalar masses, but below it for larger masses. This can be identified using the approximations in Eq. (4.2.9) and Eq. (4.2.29). For significantly large scalar masses ($\Lambda_H \gg 1, \Lambda_\tau$), the contribution in texture 4 includes an additional Λ_τ factor, resulting in an enhancement of the contribution by an order of magnitude relative to texture 1. Conversely, for small scalar masses, the extra $1/(3\Lambda_\tau)$ factor results in a reduced contribution.

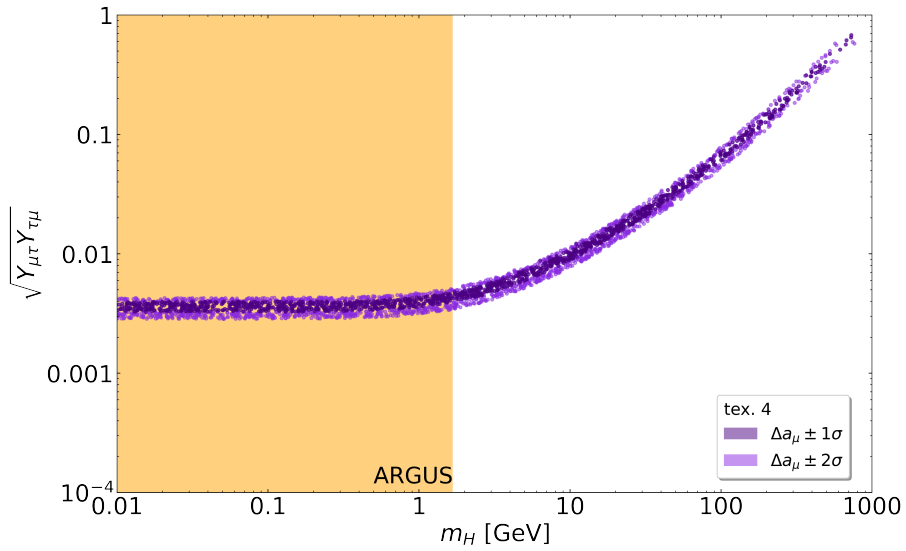

Figure 9: Possible parameter combinations to match the 1σ (dark purple) or 2σ (light purple) range of Δa_μ for texture 4. The mass hierarchy is chosen as $\Delta m = m_{A,H^+} - m_H$. The investigations at ARGUS forbid the $\tau \to \mu H$ decay, leading to the exclusion of $m_H < m_\tau - m_\mu$ (orange shaded) [29].

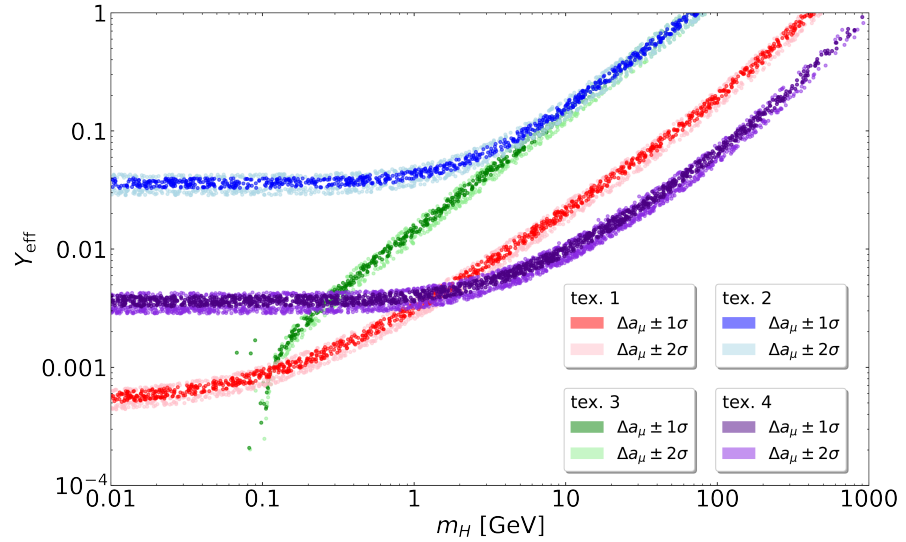

Figure 10: Illustration of possible parameter combinations within the 1σ or 2σ range of Δa_μ for the different investigated textures of the Yukawa coupling matrix. For textures 1-3, the effective Yukawa coupling Y_{eff} is given by $Y_{\ell\mu}$ with $\ell = \mu, \tau, e$. For texture 4, $Y_{\text{eff}} = \sqrt{Y_{\tau\mu}Y_{\mu\tau}}$ holds. In these scenarios, a mass hierarchy of $\Delta m = m_{A,H^+} - m_H = 110\,\text{GeV}$ is chosen.

At the end of the section, it is useful to realize that an analogous consideration with two non-vanishing Yukawa coupling elements in the electron-muon interaction scenario does not lead to any new information compared to texture 3. Due to the low electron mass, in this case, the approximation of the numerator is given by

$$x^2 - x^3 \pm \frac{m_e}{m_\mu} x^2 \approx x^2 - x^3. \tag{4.2.30}$$

With analogous scalar and pseudoscalar coefficients to Eqs. (4.2.24)-(4.2.26), the old contributions from Formulae (4.2.19) and (4.2.12) are obtained. However, for Δa_μ^ϕ, the substitution $Y_{e\mu}^2 \to Y_{e\mu}^2 + Y_{\mu e}^2$ must be made.

5 Conclusion

In this thesis, the AMM was analyzed with regard to the 2HDM. The g-factor was initially calculated using the Dirac equation and subsequently calculated using first-order time-dependent perturbation theory. This demonstrated how the identification of the muon's interaction through its magnetic moment can be derived from the invariant amplitude using Feynman diagrams. The introduction of form factors enabled a parameterized representation of the invariant amplitude. While the electric form factor provides the tree-level $g = 2$ factor due to the renormalization of the charge, the magnetic form factor indicates the anomalous magnetic moment.
This preliminary work enabled the dominant contribution from the SM, the QED one-loop correction, to be calculated. Subsequently, electroweak one-loop contributions, which include fermions and scalars, were determined for arbitrary models and checked with *Package-*`X` in *Mathematica*.

As an extension of the SM, the 2HDM was considered in the alignment limit. This implies the existence of three additional Higgs bosons beside the SM Higgs boson: a CP-even scalar H, a CP-odd scalar A, and a charged scalar H^+. In the selected Higgs basis, only a single doublet possesses a nonzero VEV, responsible for generating the masses of the charged leptons. The interaction between the fields of the second doublet and the fermion fields is governed by the Yukawa coupling matrix Y. Various textures of this Yukawa coupling were investigated.
In every scenario considered, a positive CP-even contribution was observed, which could be selected without loss of generality, along with a negative contribution from the charged scalar. Experimental data suggest that the charged scalar must not be light. A mass split of $\Delta m = m_{H^+,A} - m_H = 110\,\text{GeV}$ fulfills this requirement and additionally diminishes its negative contribution to the AMM. The CP-odd contribution exhibited varying signs across different Yukawa coupling textures but was insignificant in both cases due to the aforementioned mass split, Δm, which also prevents the $Z \to AH$ decay. Additionally, constraints from electroweak precision measurements motivated the degenerate mass of A and H^+. This thesis explored permissible parameter combinations for the mass m_H and the Yukawa coupling constant via parameter scans. It's important to note that the evaluated parameter spaces depend on the exact choice of the mass split, allowing for slight variations.
Alongside the theoretically allowed ranges, experimentally excluded ranges also exist. Specifically, the texture with a diagonal Yukawa coupling matrix has a large permissible parameter space for $m_H > 2m_\mu$, but also shows projective sensitivity ranges that may be excluded by future investigations.

The importance of the symbiotic relationship between theory and experiment became evident. Experimental observations constrain the theoretically evaluated parameter space. Therefore, we can hope for upcoming experimental results, which will further exclude parameter ranges. More accurate measurements of the magnetic moment contribute to the progress in exploring the AMM and consequently the physics BSM.
On the theoretical side, improved accuracy can also be achieved by calculating higher loop contributions. In particular, the hadronic contributions, which currently represent the largest source of theoretical uncertainty, could be determined with greater precision through lattice QCD.

A Appendix

A.1 Commutator Relation of $F(x,p)$ with p

The objective is to demonstrate that any operator function, expressible as a series expansion $F(x,p) = \sum_{n,m} c_{nm} x^n p^m$, satisfies the commutator relation:

$$[F(x,p),p] = i\frac{\partial F(x,p)}{\partial x}. \tag{A.1.1}$$

Hence, it is necessary to demonstrate

$$[x^n p^m, p] = nix^{n-1}p^m. \tag{A.1.2}$$

This can be proofed by induction. For the base case with $n = 1$ we find

$$[xp^m, p] = x[p^m, p] + [x,p]p^m = ip^m = [nix^{n-1}p^m]_{n=1}. \tag{A.1.3}$$

For the induction step $n \to n+1$ follows

$$\begin{aligned}[x^{n+1}p^m, p] &= [x,p]x^n p^m + x[x^n p^m, p] \\ &= i(n+1)x^n p^m.\end{aligned} \tag{A.1.4}$$

So the commutator relation in Eq. (A.1.2) is proven. Consequently, for an operator function that can be represented as a series expansion, we obtain Eq. (A.1.1).

A.2 The Dirac Equation

The Dirac equation in the form

$$\left(i\frac{\partial}{\partial t} + i\vec{\alpha}\cdot\vec{\nabla} - \beta m\right)\psi = 0 \tag{A.2.1}$$

can be converted into a covariant representation. This is done by multiplying the equation from left by β. As a result, with $\beta^2 = 1$, we obtain

$$\left(i\beta\frac{\partial}{\partial t} + i\beta\vec{\alpha}\cdot\vec{\nabla} - m\right)\psi = 0. \tag{A.2.2}$$

With the γ matrices

$$\gamma^\mu = (\beta, \beta\vec{\alpha}), \tag{A.2.3}$$

the covariant Dirac equation can be formulated with the slash notation $\gamma^\mu\partial_\mu = \not{\partial}$ as

$$(i\not{\partial} - m)\psi = 0. \tag{A.2.4}$$

A.3 Gordon Decomposition

The Gordon decomposition is fundamental to show that spin-$\frac{1}{2}$ particles interact via their charge and magnetic moment. The Gordon identity is given by

$$\bar{u}(q_2)\gamma^\mu u(q_1) = \frac{1}{2m}\bar{u}(q_2)\Big[(q_1+q_2)^\mu + i\sigma^{\mu\nu}(q_2-q_1)_\nu\Big]u(q_1), \tag{A.3.1}$$

with the commutator

$$\sigma^{\mu\nu} = \frac{i}{2}[\gamma^\mu, \gamma^\nu]. \tag{A.3.2}$$

This can be derived using the identities for the gamma matrices (see Appendix A.8):

$$\begin{aligned}
\bar{u}(q_2) i\sigma^{\mu\nu}(q_2 - q_1)_\nu u(q_1) &= -\frac{1}{2}\bar{u}(q_2)\Big[(\gamma^\mu\gamma^\nu - \gamma^\nu\gamma^\mu)q_{2\nu} - (\gamma^\mu\gamma^\nu - \gamma^\nu\gamma^\mu)q_{1\nu}\Big]u(q_1) \\
&= -\frac{1}{2}\bar{u}(q_2)\Big[(2g^{\mu\nu} - 2\gamma^\nu\gamma^\mu)q_{2\nu} - (2\gamma^\mu\gamma^\nu - 2g^{\mu\nu})q_{1\nu}\Big]u(q_1) \\
&= \bar{u}(q_2)\Big[\not{q}_2\gamma^\mu - q_2^\mu - q_1^\mu + \gamma^\mu\not{q}_1\Big]u(q_1) \\
&= \bar{u}(q_2)\Big[2m\gamma^\mu - (q_2 + q_1)^\mu\Big]u(q_1).
\end{aligned} \tag{A.3.3}$$

Rearranging yields the Gordon Identity.
One can establish an analogous identity incorporating γ_5:

$$\begin{aligned}
\bar{u}(q_2)\Big[i\sigma^{\mu\nu}(q_2 - q_1)_\nu\gamma_5\Big]u(q_1) &= -\frac{1}{2}\bar{u}(q_2)\Big[(\gamma^\mu\gamma^\nu - \gamma^\nu\gamma^\mu)(q_2 - q_1)_\nu\gamma_5\Big]u(q_1) \\
&= \bar{u}(q_2)\Big[(\not{q}_2\gamma^\mu - q_2^\mu - q_1^\mu + \gamma^\mu\not{q}_1)\gamma_5\Big]u(q_1) \\
&= \bar{u}(q_2)\Big[(m\gamma^\mu - (q_1 + q_2)^\mu - m\gamma^\mu)\gamma_5\Big]u(q_1) \\
&= -(q_1 + q_2)^\mu\bar{u}(q_2)\gamma_5 u(q_1).
\end{aligned} \tag{A.3.4}$$

A.4 Commutator of the Gamma Matrices

It may be helpful to write the spacial components of the commutator of the gamma matrices as

$$\sigma_{ij} = \epsilon_{ijk}\begin{pmatrix}\sigma_k & 0\\ 0 & \sigma_k\end{pmatrix}. \tag{A.4.1}$$

This result can be demonstrated using the commutator

$$[\sigma_i, \sigma_j] = 2i\epsilon_{ijk}\sigma_k \tag{A.4.2}$$

and by writing the gamma matrices in Dirac representation:

$$\begin{aligned}
\sigma_{ij} &= \frac{i}{2}[\gamma_i, \gamma_j] \\
&= \frac{i}{2}\left[\begin{pmatrix}0 & \sigma_i\\ -\sigma_i & 0\end{pmatrix}\begin{pmatrix}0 & \sigma_j\\ -\sigma_j & 0\end{pmatrix} - \begin{pmatrix}0 & \sigma_j\\ -\sigma_j & 0\end{pmatrix}\begin{pmatrix}0 & \sigma_i\\ -\sigma_i & 0\end{pmatrix}\right] \\
&= \frac{i}{2}\left[\begin{pmatrix}-\sigma_i\sigma_j & 0\\ 0 & -\sigma_i\sigma_j\end{pmatrix} - \begin{pmatrix}-\sigma_j\sigma_i & 0\\ 0 & -\sigma_j\sigma_i\end{pmatrix}\right] \\
&= -\frac{i}{2}\begin{pmatrix}[\sigma_i, \sigma_j] & 0\\ 0 & [\sigma_i, \sigma_j]\end{pmatrix} \\
&\overset{(A.4.2)}{=} \epsilon_{ijk}\begin{pmatrix}\sigma_k & 0\\ 0 & \sigma_k\end{pmatrix}.
\end{aligned} \tag{A.4.3}$$

A.5 Quantum Fields

In quantum field theory, the particles can be understood as excitations of respective quantum fields. Therefore, we use the second quantization. The operators a_p^s ($a_p^{s\dagger}$) annihilate (create) a state with momentum p and spin s. The properties of fermion fields are governed by the anticommutator algebra:

$$\{a_{p_1}^{s_1\dagger}, a_{p_2}^{s_2\dagger}\} = a_{p_1}^{s_1\dagger} a_{p_2}^{s_2\dagger} + a_{p_2}^{s_2\dagger} a_{p_1}^{s_1\dagger} = 0, \tag{A.5.1}$$

$$\{a_{p_1}^{s_1}, a_{p_2}^{s_2}\} = a_{p_1}^{s_1} a_{p_2}^{s_2} + a_{p_2}^{s_2} a_{p_1}^{s_1} = 0, \tag{A.5.2}$$

$$\{a_{p_1}^{s_1}, a_{p_2}^{s_2\dagger}\} = a_{p_1}^{s_1} a_{p_2}^{s_2\dagger} + a_{p_2}^{s_2\dagger} a_{p_1}^{s_1} = \delta_{s_1 s_2} (2\pi)^3 \delta^3(p_1 - p_2). \tag{A.5.3}$$

For bosonic fields, the corresponding commutator relations apply.
The field of real scalar particles is given by

$$\phi(x) = \int \frac{d^3p}{(2\pi)^3 \sqrt{2E_p}} \left(a_p e^{-ipx} + a_p^\dagger e^{ipx} \right). \tag{A.5.4}$$

Here, $1/\sqrt{2E_p}$ with $E_p = \sqrt{\vec{p}^2 + m^2}$ represents a conventional factor, which we have chosen in agreement with the Literature [11]. For complex scalars, on the other hand, $\phi(x) \neq \phi^*(x)$ must apply by definition. Therefore, the antiparticle creation and annihilation operators, given by $b^\dagger$ and b are introduced. The following holds:

$$\phi_c(x) = \int \frac{d^3p}{(2\pi)^3 \sqrt{2E_p}} \left(b_p e^{-ipx} + a_p^\dagger e^{ipx} \right), \tag{A.5.5}$$

$$\phi_c^*(x) = \int \frac{d^3p}{(2\pi)^3 \sqrt{2E_p}} \left(a_p e^{-ipx} + b_p^\dagger e^{ipx} \right). \tag{A.5.6}$$

There are two possible polarizations for massless photons, which results in

$$A_\mu(x) = \int \frac{d^3p}{(2\pi)^3 \sqrt{2E_p}} \sum_{\lambda=1}^{2} \left(\epsilon_\mu^\lambda(p) a_p^\lambda e^{-ipx} + \epsilon_\mu^{\lambda *}(p) a_p^{\lambda\dagger} e^{ipx} \right). \tag{A.5.7}$$

Finally, the fermion field is introduced, any Dirac field forms a superposition of $u_p^s e^{-ipx}$ and $v_p^s e^{ipx}$, where u_p^s and v_p^s are four-component spinors with spin s. The corresponding field is thus given by:

$$\psi(x) = \sum_s \int \frac{d^3p}{(2\pi)^3 \sqrt{2E_p}} \left(a_p^s u_p^s e^{-ipx} + b_p^{s\dagger} v_p^s e^{ipx} \right). \tag{A.5.8}$$

A.6 Feynman rules

Feynman rules are employed to calculate the invariant amplitudes for the associated Feynman diagrams. Subsequently, a factor is allocated to the various elements of a Feynman diagram, taken from [9]. Incoming or outgoing particles are illustrated by external lines, represented by spinors or polarization vectors, to which the following assignments are applied:

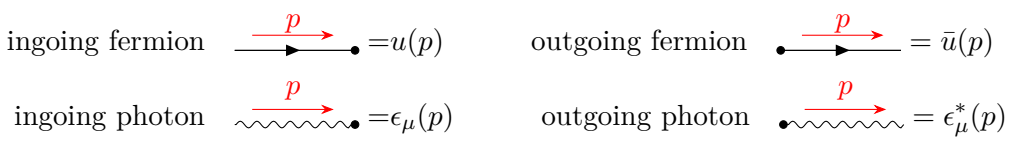

In addition to the external lines, there are also internal lines called propagators:

Boson (spin 0) 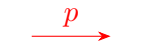 $= \dfrac{i}{p^2 - m^2}$

Fermion (spin 1/2) 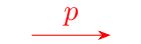 $= \dfrac{i(\not{p} + m)}{p^2 - m^2}$

Photon (spin 1) 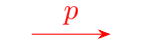 $= \dfrac{-ig^{\mu\nu}}{p^2}$

Finally, an interaction point provides a vertex factor. In QED this is given by

Photon- fermion (charge -e) 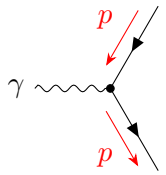 $= ie\gamma^{\mu}.$

A.7 Feynman Parameters

The Feynman parameterization serves as a technique to simplify loop integrals. It is applied to the one-loop calculations found in Section 2.4 and Section 3.1:

$$\frac{1}{ABC} = 2\int_0^1 dx\, dy\, dz \frac{\delta(x+y+z-1)}{[xA+yB+zC]^3}. \tag{A.7.1}$$

The following proof will demonstrate this. Utilize the δ-function to carry out the integration with respect to one of the variables. In this case, we commence by integrating over z:

$$\begin{aligned}
&2\int_0^1 dx \int_0^{1-x} dy \frac{1}{[xA+yB+(1-x-y)C]^3} \\
&= 2\int_0^1 dx \int_0^{1-x} dy \frac{1}{[x(A-C)+y(B-C)+C]^3} \\
&= 2\int_0^1 dx \left[\frac{-1}{2(B-C)} \frac{1}{[y(B-C)+x(A-C)+C]^2}\right]_{y=0}^{y=1-x} \\
&= \frac{1}{C-B}\int_0^1 dx \left(\frac{1}{[B+x(A-B)]^2} - \frac{1}{[C+x(A-C)]^2}\right) \\
&= \frac{1}{C-B}\left[\frac{-1}{(A-B)(B+x(A-B))} + \frac{1}{(A-C)(C+x(A-C))}\right]_{x=0}^{x=1} \\
&= \frac{1}{C-B}\left(\frac{-1}{(A-B)A} - \frac{-1}{(A-B)B} + \frac{1}{(A-C)A} - \frac{1}{(A-C)C}\right) \\
&= \frac{1}{C-B}\left(\frac{1}{AB} - \frac{1}{AC}\right) = \frac{1}{ABC}.
\end{aligned} \tag{A.7.2}$$

The limits of integration for y can be derived from the constraint given by the δ-function:

$$\begin{aligned}
\delta(x+y+z-1) &\Rightarrow z = 1-(x+y) \\
&\overset{0\leq z\leq 1}{\Rightarrow} 0 \leq (x+y) \leq 1.
\end{aligned}$$

By rearranging, we obtain a further constraint on the upper bound of the y-integration.

A.8 Gamma Matrix Identities

The characterizing property of gamma matrices is the anticommutator relation

$$\{\gamma^\mu, \gamma^\nu\} = 2g^{\mu\nu}, \tag{A.8.1}$$

where $g^{\mu\nu}$ is the Minkowski metric. Useful identities (taken from [11]) are

$$\begin{aligned} g^{\mu\nu}g_{\mu\nu} &= 4, && \text{(A.8.2)}\\ \gamma^\mu\gamma_\mu &= 4, && \text{(A.8.3)}\\ \gamma^\mu\gamma^\nu\gamma_\mu &= -2\gamma^\nu, && \text{(A.8.4)}\\ \gamma^\mu\gamma^\nu\gamma^\rho\gamma_\mu &= 4g^{\nu\rho}, && \text{(A.8.5)}\\ \gamma^\mu\gamma^\nu\gamma^\rho\gamma^\sigma\gamma_\mu &= -2\gamma^\sigma\gamma^\rho\gamma^\nu. && \text{(A.8.6)} \end{aligned}$$

Additionally, γ^5 can be defined by the expression

$$\gamma^5 = i\gamma^0\gamma^1\gamma^2\gamma^3, \tag{A.8.7}$$

which anticommutes with the gamma matrices:

$$\{\gamma^5, \gamma^\mu\} = \gamma^5\gamma^\mu + \gamma^\mu\gamma^5 = 0. \tag{A.8.8}$$

Other properties are hermiticity $(\gamma^5)^\dagger = \gamma^5$ as well as $(\gamma^5)^2 = \mathbb{I}_4$. This applies analogously to γ^0.

A.9 Momentum Integrals: Antisymmetry and Tensor Structure

Within the computations covered in Sec. 2.4 and Sec. 3.1, it was assumed that the linear terms in k disappear. In particular, this is applicable to all odd powers of k:

$$I^\mu(\Delta) = \int \frac{d^4k}{(2\pi)^4}\frac{k^{2n}k^\mu}{(k^2-\Delta)^3} = 0. \tag{A.9.1}$$

Because the integration covers the full range of k and the integrand is antisymmetric with respect to the transformation $k \to -k$, the integral sums to zero.

Within the computations, there are also integrals like

$$I^{\mu\nu}(\Delta) = \int \frac{d^4k}{(2\pi)^4}\frac{k^\mu k^\nu}{(k^2-\Delta)^3}. \tag{A.9.2}$$

Given that $I^{\mu\nu}(\Delta)$ is a tensor reliant on the scalar Δ, it must be proportional to $g^{\mu\nu}$ as it is the only tensor present in the calculation. Moreover, for consistency in dimensions, we modify $k^\mu k^\nu \to cg^{\mu\nu}k^2$. The constant c can be derived by [11, p. 830]

$$\begin{aligned} &\int \frac{d^4k}{(2\pi)^4}\frac{k^\mu k^\nu}{(k^2-\Delta)^3} = cg^{\mu\nu}\int \frac{d^4k}{(2\pi)^4}\frac{k^2}{(k^2-\Delta)^3} \qquad |\cdot g_{\mu\nu}\\ \Leftrightarrow &\int \frac{d^4k}{(2\pi)^4}\frac{k^2}{(k^2-\Delta)^3} = g_{\mu\nu}g^{\mu\nu}c\int \frac{d^4k}{(2\pi)^4}\frac{k^2}{(k^2-\Delta)^3}\\ &\overset{(A.8)}{=} 4c\int \frac{d^4k}{(2\pi)^4}\frac{k^2}{(k^2-\Delta)^3}. \end{aligned} \tag{A.9.3}$$

To fulfill the equation, $c = \frac{1}{4}$ must be chosen.

A.10 Wick Rotation

The norm of the four-vector k is determined by the Minkowski metric:

$$||k||^2 = k_0^2 - \vec{k}^2 \tag{A.10.1}$$

If k_0 can be restricted to imaginary numbers, a transition to the Euclidean metric can be made. This method can be used to prove the following integral:

$$W(\Delta) = \int \frac{d^4k}{(2\pi)^4} \frac{1}{(k^2 - \Delta + i\epsilon)^3} = -\frac{i}{32\pi^2\Delta}. \tag{A.10.2}$$

The integral has poles in the k_0 component at

$$k_0 = \sqrt{\vec{k}^2 + \Delta} - i\epsilon \qquad \text{and} \qquad k_0 = -\sqrt{\vec{k}^2 + \Delta} + i\epsilon.$$

It was used that $i\epsilon$ only describes an infinitesimal shift and thus can be excluded from the root. The procedure is illustrated in Figure 11.

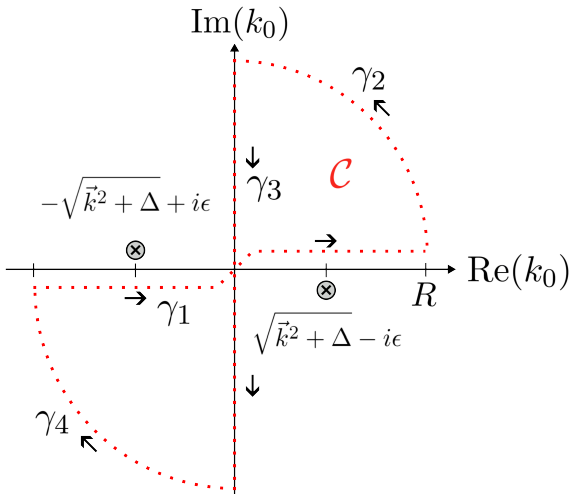

Figure 11: Illustration of the Wick rotation. The contour $\mathcal{C}$ does not enclose any poles, thus the integral over the real axis is equivalent to the integral over the imaginary axis.

Due to the Cauchy's integral theorem, the path integral of a holomorphic function $f(k_0, \vec{k})$ over a closed curve $\mathcal{C}$ disappears:

$$\oint_C f(k_0, \vec{k})\, dk_0 = 0. \tag{A.10.3}$$

Given the absence of poles within the contour $\mathcal{C}$, when the closed surface is partitioned into segments, we have:

$$\int_{\gamma_1} f(k_0, \vec{k})\, dk_0 + \int_{\gamma_2} f(k_0, \vec{k})\, dk_0 + \int_{\gamma_3} f(k_0, \vec{k})\, dk_0 + \int_{\gamma_4} f(k_0, \vec{k})\, dk_0 = 0. \tag{A.10.4}$$

Since the integrand diminishes to zero as $|k_0| \to \infty$, the contour integrals along γ_2 and γ_4 become insignificant as $R \to \infty$ (see Fig. 11). Therefore, this results in:

$$\int_{-\infty}^{\infty} f(k_0, \vec{k})\, dk_0 + \int_{i\infty}^{-i\infty} f(k_0, \vec{k})\, dk_0 = 0. \tag{A.10.5}$$

Hence, the integral can be resolved by employing the Euclidean metric. With the substitution $k_0 = ik_{0,E}$ (and $\vec{k} = \vec{k}_E$) we obtain

$$W(z) = -i \int \frac{d^4 k_E}{(2\pi)^4} \frac{1}{(k_E^2 + \Delta)^3}. \tag{A.10.6}$$

The integral over the angles of a 4-dimensional sphere yields $2\pi^2$, thus it remains to carry out the radial integral:

$$W(z) = -i \frac{2\pi^2}{16\pi^4} \int_0^\infty dk_E \, \frac{k_E^3}{(k_E^2 + \Delta)^3} \tag{A.10.7}$$

Through the substitution $z = k_E^2 + \Delta$, the integral expression can be performed:

$$\begin{aligned} W(z) = -\frac{i}{8\pi^2} \int_\Delta^\infty dz \frac{1}{2} \frac{z - \Delta}{z^3} &= -\frac{i}{16\pi^2} \left[-\frac{1}{z} + \frac{\Delta}{2z^2} \right]_\Delta^\infty \\ &= -\frac{i}{16\pi^2} \left(\frac{1}{\Delta} - \frac{1}{2\Delta} \right) = -\frac{i}{32\pi^2 \Delta}. \end{aligned} \tag{A.10.8}$$

A.11 The Right-Handed and Left-Handed Projection Operators

As mentioned in Sec. 2.1, in the Weyl representation of the Dirac equation, the mass couples the upper two and lower two components of the four-component spinor. These components are called left-handed and right-handed Weyl spinors. Consequently, in this representation holds:

$$\psi = \begin{pmatrix} \psi_L \\ \psi_R \end{pmatrix}. \tag{A.11.1}$$

They correspond to either the $(\frac{1}{2}, 0)$ or $(0, \frac{1}{2})$ representation of the Lorentz group. Therefore, they transform independently under Lorentz transformations [35, p. 85]. The γ^5 matrix in the Weyl representation is given by

$$\gamma^5 = \begin{pmatrix} -\mathbb{I}_2 & 0 \\ 0 & \mathbb{I}_2, \end{pmatrix}, \tag{A.11.2}$$

where ψ_L and ψ_R are the corresponding eigenstates associated with eigenvalues -1 and $+1$. Consequently, the idempotent projectors can be defined as

$$P_L = \frac{1 - \gamma^5}{2} \qquad \text{and} \qquad P_R = \frac{1 + \gamma^5}{2}, \tag{A.11.3}$$

fulfilling the properties $P_L \psi = \psi_L$ and $P_R \psi = \psi_R$.

A.12 Verification of Fermion-Scalar Contributions to the Anomalous Magnetic Moment using Package-X

In the following, the analytical calculation from Section 3 will be verified using the publicly accessible *Package-*`X` [6] in *Mathematica*. The effect of photoemission from the charged scalar line on the anomalous magnetic moment will also be computed using a analogous approach.
In the respective one-loop calculations, different scalar products occur between four momenta. Due to the on-shell conditions, the following substitutions apply:

```
In[1]:= onShell = {q1.q1→m_μ^2, q2.q2→m_μ^2, q1.q2→m_μ^2 - p.p/2, p.q1→-p.p/2, p.q2→p.p/2};
```

Feynman parameters will be utilized as Lorentz scalars to simplify the denominator. In addition, **substitutionRule** is introduced to perform the $k^\mu \to k^\mu - yp + zq_1$ shift performed in the calculation:

```
In[2]:= LScalarQ[x] = True;
        LScalarQ[y] = True;
        LScalarQ[z] = True;
        substitutionRule = a_.k: →a.(k-y p+z q1);
```

Photoemission from the charged Fermion Line

The numerator and denominator of the integrand of the invariant amplitude $\mathcal{M}$, given in Eq. (3.1.1), will be transformed separately in the following. For the numerator, the function **FermionLineExpand** is used, whereby the products of the gamma matrices are expanded between the on-shell spinors ***u*[q,m]**. The Dirac equation is applied, and the expression is then modified using the Gordon identities. We therefore use the following code for the numerator:

```
In[3]:= Num = Simplify[FermionLineExpand[⟨u[q2,m_μ],Cs 1+Cp γ5,
            γ.p+γ.k+m_F 1,γ_μ,γ.k+m_F 1,
            Conjugate[Cs] 1-Conjugate[Cp] γ5,u[q1,m_μ]⟩
            /. substitutionRule/. onShell]];
        FullSimplify[Coefficient[Num
             /. {p→q2-q1},⟨u[q2,m_μ],σ_μ,{-q1+q2},u[q1,m_μ]⟩]/. {p→0}]

Out[3]= -i (-1+z) (Cp Conjugate[Cp] (-m_F+z m_μ)+Cs Conjugate[Cs] (m_F+z m_μ))
```

The function **Coefficient** only filters the numerator according to the term including $\langle u[q2,m_\mu],\sigma_{\mu,\{-q1+q2\}},u[q1,m_\mu]\rangle$, which is decisive for the magnetic moment.
Analogue to the calculation in Sec. 3, the denominator is first rewritten using the Feynman parameters and the corresponding factors a, b and c:

```
In[4]:= a = k.k-m_F^2;
        b =(p+k).(p+k)-m_F^2;
        c = (k-q1).(k-q1)-m_H^2;
        Denum = Simplify[Expand[x a+y b+z c+i ϵ]];
        Denum = Denum/. onShell/. {x+y+z→1}

Out[4]= i ϵ+k.k+2 y k.p-2 z k.q1+y p.p-x m_F^2-y m_F^2-z m_H^2+z m_μ^2
```

By performing the integration via Wick Rotation, the denominator is represented by Δ as outlined in Eq. (2.4.38) with $p^2 = 0$. The code below was utilized to find this expression:

```
In[5]:= CompareTerm = Expand[(k+y p-z q1).(k+y p-z q1)+i ϵ];
        CompareTerm = CompareTerm/. onShell/. {x+y+z→1};
        Δ = CompareTerm-Denum;
        Collect[Δ,{m_μ^2,m_F^2,m_H^2}]/. {x+y→1-z,p.p→0}

Out[5]= (1-z) m_F^2+z m_H^2+(-z+z^2) m_μ^2
```

Overall, this results in

$$F_M(0) = -2eQ_F \frac{-i}{32\pi^2}\frac{2m_\mu}{e} \times \int_0^1 dz \int_0^{1-z} dy \, \frac{-i(z-1)\Big[(m_F+zm_\mu)|C_S|^2 + (-m_F+zm_\mu)|C_P|^2\Big]}{(1-z)m_F^2 + zm_H^2 + (-z+z^2)m_\mu^2}. \tag{A.12.1}$$

The prefactors arise from Eq. (3.1.9), the momentum integration through Wick rotation and the identification of the magnetic form factor from $i\mathcal{M}^\mu$ (see Eq. (2.3.10)). In summary, after the y-integration and the $z \to 1-z$ substitution we get

$$F_M(0) = -\frac{Q_F}{8\pi^2}\int_0^1 dz \, \frac{\Big(z^2(1-z)+\Lambda_F z^2\Big)|C_S|^2 + \Big(z^2(1-z)-\Lambda_F z^2\Big)|C_P|^2}{z^2 + z(\Lambda_F^2-1) + \Lambda_H^2(1-z)}, \tag{A.12.2}$$

where $\Lambda_i = m_i/m_\mu$ applies for $i = F, H$.

Photoemission from the Charged Scalar Line

The contribution, characterized by the Feynman diagram with the photoemission from the internal charged scalar line, can be determined analogously. The result for the numerator is determined by

```
In[6]:= Num = Simplify[FermionLineExpand[⟨u[q2,mμ],Cs 1+Cp γ5,
            γ.q1-γ.k+mF 1,2 kμ 1+pμ 1,
            Conjugate[Cs] 1-Conjugate[Cp] γ5,u[q1,mμ]⟩
            /.kμ→kμ-y pμ+z q1μ/.substitutionRule/.onShell]];
        Simplify[Coefficient[Num,⟨u[q2,mμ],σμ,{-q1+q2},u[q1,mμ]⟩]/.{p→0}]

Out[6]= i z ((Cp Conjugate[Cp]-Cs Conjugate[Cs]) mF
        +(-1+z) (Cp Conjugate[Cp]+Cs Conjugate[Cs]) mμ)
```

In this case, the denominator is given by:

```
In[7]:= a = k.k-mH^2;
        b = (p+k).(p+k)-mH^2;
        c = (k-q1).(k-q1)-mF^2;

        Denum = Simplify[Expand[x a+y b+z c+i ϵ]];
        Denum = Denum/.onShell/.{x+y+z→1};
        Δ = CompareTerm-Denum;
        Collect[Δ,{mμ^2,mF^2,mH^2}]/.{x+y→1-z,p→0}

Out[7]= z mF^2+(1-z) mH^2+(-z+z^2) mμ^2
```

Here we used **CompareTerm**, which is already defined. Overall, this results in

$$F_M(0) = -2eQ_H \frac{-i}{32\pi^2}\frac{2m_\mu}{e} \times \int_0^1 dz \int_0^{1-z} \frac{iz\Big((|C_P|^2-|C_S|^2)m_F + (-1+z)(|C_P|^2+|C_S|^2)m_\mu\Big)}{zm_F^2 + (1-z)m_H^2 + (-z+z^2)m_\mu^2}. \tag{A.12.3}$$

After performing the y-integration, as well as the substitution $z \to 1-z$, the result follows as

$$F_M(0) = -\frac{Q_H}{8\pi^2}\int_0^1 dz\, \frac{\Big(z^2(z-1)+\Lambda_F(z^2-z)\Big)|C_S|^2 + \Big(z^2(z-1)-\Lambda_F(z^2-z)\Big)|C_P|^2}{z^2+\Lambda_F^2(1-z)+z(\Lambda_H^2-1)}. \tag{A.12.4}$$

A.13 Scalar Mass Matrix in the Two-Higgs-Doublet Model

In the following, the mass matrix in the Higgs basis, with the potential in Eq. (4.1.3) will be derived. Subsequent diagonalization leads to mass eigenstates with the corresponding eigenvalues. At the potential's minimum, the doublets achieve their VEVs. Thus, the minimization condition is defined by $\partial\mathcal{V}/\partial H_1 = 0$ and $\partial\mathcal{V}/\partial H_2 = 0$ evaluated at $\langle H_1\rangle = v/\sqrt{2}$ and $\langle H_2\rangle = 0$. This leads to

$$m_{11}^2 = -\frac{1}{2}v^2\lambda_1 \qquad \text{and} \qquad m_{12}^2 = \frac{1}{2}v^2\lambda_6. \tag{A.13.1}$$

The mass matrix of the charged scalars can be represented as

$$\mathcal{M}_c^2 = \begin{pmatrix} \frac{\partial^2\mathcal{V}}{\partial H^+\partial H^-} & \frac{\partial^2\mathcal{V}}{\partial H^+\partial G^-} \\ \frac{\partial^2\mathcal{V}}{\partial G^+\partial H^-} & \frac{\partial^2\mathcal{V}}{\partial G^+\partial G^-} \end{pmatrix} = \begin{pmatrix} m_{22}^2 + \frac{1}{2}v^2\lambda_3 & 0 \\ 0 & 0 \end{pmatrix}. \tag{A.13.2}$$

The matrix is already diagonalized, leading to

$$m_{H^+} = m_{22}^2 + \frac{1}{2}v^2\lambda_3 \qquad \text{and} \qquad m_{G^+} = 0. \tag{A.13.3}$$

Therefore, G^+ can be identified as a Goldstone Boson. Based on the minimization conditions, the mass matrix for the neutral scalars is given by

$$\begin{aligned}\mathcal{M}_n^2 &= \left(\frac{\partial^2\mathcal{V}}{\partial\phi_i\partial\phi_j}\right)_{\phi_i,\phi_j = H_1^0, H_2^0, A^0, G^0} \\ &= \begin{pmatrix} \lambda_1 v^2 & \mathrm{Re}(\lambda_6)v^2 & -\mathrm{Im}(\lambda_6)v^2 & 0 \\ \mathrm{Re}(\lambda_6)v^2 & m_{22}^2 + \frac{1}{2}v^2(\lambda_3+\lambda_4+\mathrm{Re}(\lambda_5)) & -\frac{1}{2}\mathrm{Im}(\lambda_5)v^2 & 0 \\ -\mathrm{Im}(\lambda_6)v^2 & -\frac{1}{2}\mathrm{Im}(\lambda_5)v^2 & m_{22}^2 + \frac{1}{2}v^2(\lambda_3+\lambda_4-\mathrm{Re}(\lambda_5)) & 0 \\ 0 & 0 & 0 & 0 \end{pmatrix}.\end{aligned} \tag{A.13.4}$$

Consequently, also G^0 is a Goldstone Boson. The assumption of CP-conservation leads to real parameters, whereby the CP-odd eigenstate, due to the block diagonal form, decouples and a mass of

$$m_A^2 = m_{22}^2 + \frac{1}{2}v^2(\lambda_3+\lambda_4-\mathrm{Re}(\lambda_5)) \tag{A.13.5}$$

$$= m_{H^+}^2 - \frac{1}{2}v^2(\lambda_5-\lambda_4) \tag{A.13.6}$$

is obtained. The eigenvalues of the CP-even scalars result from the corresponding 2×2 matrix, labeled as $\mathcal{M}_{2\times 2}$:

$$m_{h,H}^2 = \frac{1}{2}\left(\mathrm{tr}[\mathcal{M}_{2\times 2}] \mp \sqrt{\mathrm{tr}^2[\mathcal{M}_{2\times 2}] - 4\det[\mathcal{M}_{2\times 2}]}\right)$$

$$= \frac{1}{2}\left(m_A^2 + v^2(\lambda_1+\lambda_5) \mp \sqrt{[m_A^2 + (\lambda_1+\lambda_5)v^2]^2 - 4\lambda_1 v^2(m_A^2+\lambda_5 v^2) + 4\lambda_6^2 v^4}\right)$$
$$= \frac{1}{2}\Big[m_A^2 + v^2(\lambda_1+\lambda_5) \mp \sqrt{[m_A^2 + (\lambda_5-\lambda_1)v^2]^2 + 4\lambda_6^2 v^4}\Big]. \tag{A.13.7}$$

Since the eigenstates of a real symmetric matrix are orthogonal, a rotation matrix can be used to transform into the eigenstates:

$$\begin{pmatrix} h \\ H \end{pmatrix} = \begin{pmatrix} \cos(\alpha-\beta) & \sin(\alpha-\beta) \\ -\sin(\alpha-\beta) & \cos(\alpha-\beta) \end{pmatrix} \begin{pmatrix} H_1^0 \\ H_2^0 \end{pmatrix}. \tag{A.13.8}$$

Here we use the convention of the rotation angle $\alpha-\beta$, since the Higgs basis considered here is already a basis rotated by the angle β. The required rotation angle for diagonalization is determined by

$$\sin 2(\alpha-\beta) = \frac{2\Lambda_6 v^2}{m_H^2 - m_h^2}. \tag{A.13.9}$$

Under the alignment limit being considered, where $\alpha \approx \beta$, it follows $\lambda_6 = 0$ and therefore:

$$m_h^2 = \lambda_1 v^2, \qquad m_H^2 = m_{22}^2 + \frac{v^2}{2}(\lambda_3+\lambda_4+\lambda_5), \tag{A.13.10}$$

$$m_A^2 = m_H^2 - v^2\lambda_5, \qquad m_{H^\pm}^2 = m_H^2 - \frac{v^2}{2}(\lambda_4+\lambda_5). \tag{A.13.11}$$

This result is cross-checked with [36].

A.14 Integrals needed for Approximations of Δa_μ

In Section 4.2, the effects of various textures in the Yukawa coupling were estimated for both large and small scalar masses. The approximation for large neutral scalar masses $\Lambda_\phi \gg 1$ in the diagonal coupling case (texture 1), as well as in the scenario with two off-diagonal Yukawa coupling elements (texture 4), is non-trivial.
In texture 1, the CP-even scalar contribution is given by:

$$\Delta a_\mu^H = \frac{Y_{\mu\mu}}{16\pi^2}\int_0^1 dz\, \frac{z^2(2-z)}{z^2 + \Lambda_H^2(1-z)}. \tag{A.14.1}$$

For $\Lambda_H \gg 1$, the term z^2 can be ignored unless $z \to 1$. Within this limit, the Λ_H^2 term vanishes, leading to the approximation:

$$\Delta a_\mu^H \approx \frac{Y_{\mu\mu}}{16\pi^2}\int_0^1 dz\, \frac{z^2(2-z)}{1 + \Lambda_H^2(1-z)}. \tag{A.14.2}$$

The substitution $u = 1 + \Lambda_H^2(1-z)$ results in

$$\Delta a_\mu^H \approx \frac{Y_{\mu\mu}}{16\pi^2}\int_{1+\Lambda_H^2}^1 du\, \frac{\left(\frac{u-1-\Lambda_H^2}{\Lambda_H^2}\right)^2\left(\frac{u-1+\Lambda_H^2}{\Lambda_H^2}\right)}{-u\Lambda_H^2} \tag{A.14.3}$$

$$= \frac{Y_{\mu\mu}}{16\pi^2}\Big(-\frac{1}{\Lambda_H^8}\Big)\int_{1+\Lambda_H^2}^1 du \frac{(u-1-\Lambda_H^2)^2(u-1+\Lambda_H^2)}{u} \tag{A.14.4}$$

$$\approx \frac{Y_{\mu\mu}}{16\pi^2}\frac{1}{\Lambda_H^2}\ln\Lambda_H^2. \tag{A.14.5}$$

Due to the linearity of the integral, the individual terms can be integrated after substitution. In the last step, only the dominant term for large scalar masses ($\Lambda_H \gg 1$) was taken into account. The derivations for Eq. (4.2.11) and Eq. (4.2.29) can be done in a similar manner. It should be noted that in the second case the increased restriction $\Lambda_\phi \gg \Lambda_\tau$ is required.

References

[1] Mark Trodden. *Electroweak Baryogenesis: A Brief Review*. 1998. arXiv: hep-ph/9805252 [hep-ph].

[2] T. Aoyama et al. "The anomalous magnetic moment of the muon in the Standard Model". In: *Physics Reports* 887 (Dec. 2020), pp. 1–166. ISSN: 0370-1573. DOI: 10.1016/j.physrep.2020.07.006.

[3] D. P. Aguillard et al. "Measurement of the Positive Muon Anomalous Magnetic Moment to 0.20 ppm". In: *Physical Review Letters* 131.16 (Oct. 2023). ISSN: 1079-7114. DOI: 10.1103/physrevlett.131.161802.

[4] B. Abi et al. "Measurement of the Positive Muon Anomalous Magnetic Moment to 0.46 ppm". In: *Physical Review Letters* 126.14 (Apr. 2021). ISSN: 1079-7114. DOI: 10.1103/physrevlett.126.141801.

[5] G. W. Bennett et al. "Final report of the E821 muon anomalous magnetic moment measurement at BNL". In: *Physical Review D* 73.7 (Apr. 2006). ISSN: 1550-2368. DOI: 10.1103/physrevd.73.072003.

[6] Hiren H. Patel. "Package-X: A Mathematica package for the analytic calculation of one-loop integrals". In: *Computer Physics Communications* 197 (Dec. 2015), pp. 276–290. ISSN: 0010-4655. DOI: 10.1016/j.cpc.2015.08.017.

[7] M. C. Rodriguez. *The Minimal Supersymmetric Standard Model (MSSM) and General Singlet Extensions of the MSSM (GSEMSSM), a short review*. 2019. arXiv: 1911.13043 [hep-ph].

[8] Philipp Basler, Margarete Mühlleitner, and Jonas Müller. *Electroweak Baryogenesis in the CP-Violating Two-Higgs Doublet Model*. 2021. arXiv: 2108.03580 [hep-ph].

[9] Francis Halzen and Alan Martin. *Quarks & Leptons: An introductory course in modern particle physics*. New York, USA: John Wiley & Sons, 1984.

[10] W. Nolting. *Grundkurs Theoretische Physik 5/2: Quantenmechanik - Methoden und Anwendungen*. Grundkurs Theoretische Physik. Springer Berlin Heidelberg, 2007. ISBN: 9783540476160.

[11] Matthew D. Schwartz. *Quantum Field Theory and the Standard Model*. Cambridge University Press, 2013.

[12] Fred Jegerlehner and Andreas Nyffeler. *The Muon g-2*. Feb. 2009. arXiv: 0902.3360.

[13] Julian Schwinger. "On Quantum-Electrodynamics and the Magnetic Moment of the Electron". In: *Phys. Rev.* 73 (4 Feb. 1948), pp. 416–417. DOI: 10.1103/PhysRev.73.416.

[14] Bingrong Yu and Shun Zhou. "General remarks on the one-loop contributions to the muon anomalous magnetic moment". In: *Nuclear Physics B* 975 (Feb. 2022), p. 115674. ISSN: 0550-3213. DOI: 10.1016/j.nuclphysb.2022.115674.

[15] G.C. Branco et al. "Theory and phenomenology of two-Higgs-doublet models". In: *Physics Reports* 516.1–2 (July 2012), pp. 1–102. ISSN: 0370-1573. DOI: 10.1016/j.physrep.2012.02.002.

[16] H.E. Haber and G.L. Kane. "The search for supersymmetry: Probing physics beyond the standard model". In: *Physics Reports* 117.2 (1985), pp. 75–263. ISSN: 0370-1573. DOI: https://doi.org/10.1016/0370-1573(85)90051-1.

[17] G. C. Branco et al. *Theory and phenomenology of two-Higgs-doublet models*. July 2012. DOI: 10.1016/j.physrep.2012.02.002.

[18] M. Tanabashi et al. "Review of Particle Physics". In: *Phys. Rev. D* 98 (3 Aug. 2018), p. 030001. DOI: 10.1103/PhysRevD.98.030001.

[19] Particle Data Group. *$H^{\pm}$ (charged Higgs) mass limits webpage*. http://pdglive.lbl.gov/DataBlock.action?node=S064HGC&init=. [Accessed: September 2024].

[20] Sudip Jana, Vishnu P. K., and Shaikh Saad. "Resolving electron and muon $g-2$ within the 2HDM". In: *Phys. Rev. D* 101 (11 June 2020), p. 115037. DOI: 10.1103/PhysRevD.101.115037.

[21] F. Arco, S. Heinemeyer, and M. J. Herrero. "Exploring sizable triple Higgs couplings in the 2HDM". In: *The European Physical Journal C* 80.9 (Sept. 2020). ISSN: 1434-6052. DOI: 10.1140/epjc/s10052-020-8406-8.

[22] K. S. Babu, Sudip Jana, and Vishnu P. K. "Correlating W-Boson Mass Shift with Muon $g-2$ in the Two Higgs Doublet Model". In: *Phys. Rev. Lett.* 129 (12 Sept. 2022), p. 121803. DOI: 10.1103/PhysRevLett.129.121803.

[23] Pauli Virtanen et al. "SciPy 1.0: fundamental algorithms for scientific computing in Python". In: *Nature Methods* 17.3 (Feb. 2020), pp. 261–272. ISSN: 1548-7105. DOI: 10.1038/s41592-019-0686-2.

[24] J. D. Bjorken et al. "Search for neutral metastable penetrating particles produced in the SLAC beam dump". In: *Phys. Rev. D* 38 (11 Dec. 1988), pp. 3375–3386. DOI: 10.1103/PhysRevD.38.3375.

[25] A. M. Sirunyan et al. "Search for an Lμ − Lτ gauge boson using Z $\to 4\mu$ events in proton-proton collisions at s=13 TeV". In: *Physics Letters, Section B: Nuclear, Elementary Particle and High-Energy Physics* 792 (May 2019), pp. 345–368. ISSN: 03702693. DOI: 10.1016/j.physletb.2019.01.072.

[26] J. P. Lees et al. "Search for a muonic dark force atBaBar". In: *Physical Review D* 94.1 (July 2016). ISSN: 2470-0029. DOI: 10.1103/physrevd.94.011102.

[27] T. Abe et al. *Belle II Technical Design Report*. 2010. arXiv: 1011.0352 [physics.ins-det].

[28] Brian Batell et al. "Flavor-specific scalar mediators". In: *Physical Review D* 98.5 (Sept. 2018). ISSN: 2470-0029. DOI: 10.1103/physrevd.98.055026.

[29] H. Albrecht et al. "A search for the lepton-flavour violating decays $\tau \to e\alpha$, $\tau \to \mu\alpha$" in: *Zeitschrift für Physik C Particles and Fields* 68.1 (1995), pp. 25–28. DOI: 10.1007/BF01579801.

[30] Rahool Kumar Barman, Ritu Dcruz, and Anil Thapa. "Neutrino masses and magnetic moments of electron and muon in the Zee Model". In: *Journal of High Energy Physics* 2022.3 (Mar. 2022). ISSN: 1029-8479. DOI: 10.1007/jhep03(2022)183.

[31] A. Hayrapetyan et al. "Search for the lepton-flavor violating decay of the Higgs boson and additional Higgs bosons in the $e\mu$ final state in proton-proton collisions at $\sqrt{s} = 13$ TeV". In: *Phys. Rev. D* 108 (7 Oct. 2023), p. 072004. DOI: 10.1103/PhysRevD.108.072004.

[32] Particle Data Group et al. "Review of Particle Physics". In: *Progress of Theoretical and Experimental Physics* 2022.8 (Aug. 2022), p. 083C01. ISSN: 2050-3911. DOI: 10.1093/ptep/ptac097. eprint: https://academic.oup.com/ptep/article-pdf/2022/8/083C01/49175539/ptac097.pdf.

[33] Johannes Herms et al. “Minimal Realization of Light Thermal Dark Matter”. In: *Physical Review Letters* 129.9 (Aug. 2022). ISSN: 1079-7114. DOI: 10.1103/physrevlett.129.091803.

[34] Yoav Afik, P. S. Bhupal Dev, and Anil Thapa. “Hints of a new leptophilic Higgs sector?” In: *Physical Review D* 109.1 (Jan. 2024). ISSN: 2470-0029. DOI: 10.1103/physrevd.109.015003.

[35] Jakob Schwichtenberg. *Physics from Symmetry*. Undergraduate Lecture Notes in Physics. Springer, 2018. ISBN: 978-3-319-19201-7, 978-3-319-66630-3, 978-3-319-88288-8, 978-3-319-66631-0. DOI: 10.1007/978-3-319-66631-0.

[36] K. S. Babu and Sudip Jana. “Enhanced di-Higgs production in the two Higgs doublet model”. In: *Journal of High Energy Physics* 2019.2 (Feb. 2019). ISSN: 1029-8479. DOI: 10.1007/jhep02(2019)193.

Declaration of Academic Integrity

I hereby confirm that this thesis, entitled _____

_____ is solely my own work and that I have used no sources or aids other than the ones stated. All passages in my thesis for which other sources, including electronic media, have been used, be it direct quotes or content references, have been acknowledged as such and the sources cited. I am aware that plagiarism is considered an act of deception which can result in sanction in accordance with the examination regulations.

_____
(date, signature of student)

I consent to having my thesis cross-checked with other texts to identify possible similarities and to having it stored in a database for this purpose.

I confirm that I have not submitted the following thesis in part or whole as an examination paper before.

_____
(date, signature of student)